1.0

1.1

1.25 1.4 1.6

4.5
5.0
5.6
6.3

2.8 2.5

3.2 2.2

3.6

4.0 2.0

1.8

MICROCOPY RESOLUTION TEST CHART
NATIONAL BUREAU OF STANDARDS-1963-A

department of electrical engineering

CSU
1870

8

ARO 13279.1-MS

A Comparison of Dipole and Finite Element

Models for Predicting Leakage Fields Around

Rectangular Slots in Ferromagnetic Materials

ARO Technical Report

January 1978

DDC

RECEIVED

MAY 3 1978

D

W. Lord, Principal Investigator
Electrical Engineering Department
Colorado State University
Fort Collins, CO 80523
Telephone: (303) 491-6018 (or 6706)

8

A Comparison of Dipole and Finite Element Models for Predicting

Leakage Fields Around Rectangular Slots in Ferromagnetic Materials

W. Lord, J. M. Bridges, W. Yen and

R. Palanisamy

ARO Technical Report

January 1978

D D C

RECEIVED

MAY 3 1978

D

W. Lord, Principal Investigator
Electrical Engineering Department
Colorado State University
Fort Collins, CO 80523
Telephone: (303) 491-6018 (or 6706)

SECURITY CLASSIFICATION OF THIS PAGE (When Data Entered)

ARO 13279.1-MS

REPORT DOCUMENTATION PAGE	READ INSTRUCTIONS BEFORE COMPLETING FORM

1. REPORT NUMBER	2. 3OVT ACCESSION NO.	3. RECIPIENT'S CATALOG NUMBER
13279.1-MS		

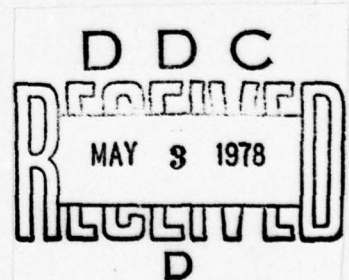| 4. TITLE (and Subtitle)	5. TYPE OF REPORT & PERIOD COVERED
A Comparison of Dipole and Finite Element Models for Predicting Leakage Fields Around Rectangular Slots in Ferromagnetic Materials	Technical Report
	6. PERFORMING ORG. REPORT NUMBER

7. AUTHOR(s)	8. CONTRACT OR GRANT NUMBER(s)
W. Lord W. Yen J. M. Bridges R. Palanisamy	DAAG29 76 G 0249

9. PERFORMING ORGANIZATION NAME AND ADDRESS	10. PROGRAM ELEMENT, PROJECT, TASK AREA & WORK UNIT NUMBERS
Colorado State University Fort Collins, Colorado 80523	

11. CONTROLLING OFFICE NAME AND ADDRESS	12. REPORT DATE
U. S. Army Research Office Post Office Box 12211 Research Triangle Park, NC 27709	January 1978
	13. NUMBER OF PAGES
	29

14. MONITORING AGENCY NAME & ADDRESS(if different from Controlling Office)	15. SECURITY CLASS. (of this report)
	Unclassified
	15a. DECLASSIFICATION/DOWNGRADING SCHEDULE

16. DISTRIBUTION STATEMENT (of this Report)

Approved for public release; distribution unlimited.

17. DISTRIBUTION STATEMENT (of the abstract entered in Block 20, if different from Report)

18. SUPPLEMENTARY NOTES

The findings in this report are not to be construed as an official Department of the Army position, unless so designated by other authorized documents.

19. KEY WORDS (Continue on reverse side if necessary and identify by block number)

Computerized simulation	Crystal defects	Magnetization
Dipoles	Interactions	
Finite element	Nondestructive testing	
Mathematical models	Steel	
Magnetic fields	Computer programs	

20. ABSTRACT (Continue on reverse side if necessary and identify by block number)

This technical report describes computer code generated for the study of dipole and finite element models of magnetic field/defect interactions associated with leakage field methods of nondestructive testing. It is the principal investigator's contention that finite element analysis techniques could be used to develop defect characterization shcemes for all electromagnetic methods of nondestructive testing, as well as providing valuable insight into the study of defect signal phenomena. Experimental results are given, showing Hall probe generated leakage field profiles

DD FORM 1 JAN 73 1473   EDITION OF 1 NOV 65 IS OBSOLETE

SECURITY CLASSIFICATION OF THIS PAGE (When Data Entered)

20. ABSTRACT CONTINUED

around rectangular slots in a steel bar, and compared with both dipole and finite element model predictions. The finite element code has already been used to produce a library of leakage field profiles for a variety of surface and subsurface defects in a ferromagnetic bar carrying an axial dc magnetizing current and as part of ARO Grant DAAG29-76-G-0249, the code will be extended to include residual forms of magnetization.

Contents

Abstract

This technical report describes computer code generated for the study of dipole and finite element models of magnetic field/defect interactions associated with leakage field methods of nondestructive testing. It is the principal investigator's contention that finite element analysis techniques could be used to develop defect characterization schemes for all electromagnetic methods of nondestructive testing, as well as providing valuable insight into the study of defect signal phenomena.

Experimental results are given, showing Hall probe generated leakage field profiles around rectangular slots in a steel bar, and compared with both dipole and finite element model predictions. The finite element code has already been used to produce a library of leakage field profiles for a variety of surface and subsurface defects in a ferromagnetic bar carrying an axial dc magnetizing current and as part of ARO contract DAAG29-76-G-0249, the code will be extended to include residual forms of magnetization.

Introduction

During the past decade, the urgent need for incorporating nondestructive testing and evaluation considerations directly into the engineering design process has been amply illustrated by material failures in aerospace, electric pcwer and transportation industry equipment. The economic impact of such failures is well documented[1-4] and provides a major impetus to improve all aspects of the nondestructive testing art. Considerable progress has been made toward this end through such efforts as the ARPA/ AFML program[5]. Although the work has concentrated primarily on ultrasonic techniques, much of the research philosophy developed for the program with regard to the study of basic phenomena[6], development of models[7], signature identification by signal processing[8] and the subsequent accept/ reject decision founded on a knowledge of fracture mechanics and related failure probabilities could and should be applied to other nondestructive testing techniques. The cornerstone of such an approach is the development of an adequate mathematical model for the study of the basic field/ defect interactions. Such a model is needed in order to develop a defect characterization scheme and to identify suitable parameters for the signal processing.

Despite recent developments in automatic defect characterization associated with eddy current and leakage flux methods of nondestructive testing[9,10], the subject of electromagnetic methods of nondestructively testing ferromagnetic materials is characterized largely by empirical knowledge. Where closed form mathematical solutions do exist, describing electromagnetic field/defect interactions, the underlying assumptions of the theories tend to invalidate any realistic application of the results

to the problem of defect characterization in ferromagnetic materials.

The problem of modeling electromagnetic field/defect interactions in ferromagnetic materials is complicated not only by the nonlinear magnetization characteristic of the material and the awkward defect boundaries but also by the number of different phenomena utilized[11]. Figure 1 shows the three major modes of field/defect interaction. In magnetic particle and magnetographic methods of nondestructive testing, the ferromagnetic specimen to be tested is initially magnetized with dc current. Residual leakage fields are set up around defects present in the specimen. The presence of such fields can be observed either directly using magnetic particles or indirectly by recording the leakage fields on magnetic tape. With reluctance and perturbation techniques, a constant dc magnetization current is used to set up active leakage fields around defects in the parts undergoing inspection, which can be detected using any flux sensitive transducer[11]. Finally in eddy current testing, ac excitation is used to induce secondary currents and fields in the specimen. In this case the presence of a defect causes changes in both induced currents and fields, resulting in measurable impedance variations in the pick-up coil.

Differences in the residual, active and eddy phenomena are summarized in Figure 1 which shows the regions of the material's B-H characteristic over which the various phenomena occur.

The major purpose of this technical report is to give details of a finite element model for predicting leakage fields around defects in ferromagnetic parts carrying dc magnetization current. It is the principal investigators contention that the finite element model could be used as the basis for developing defect characterization schemes for all
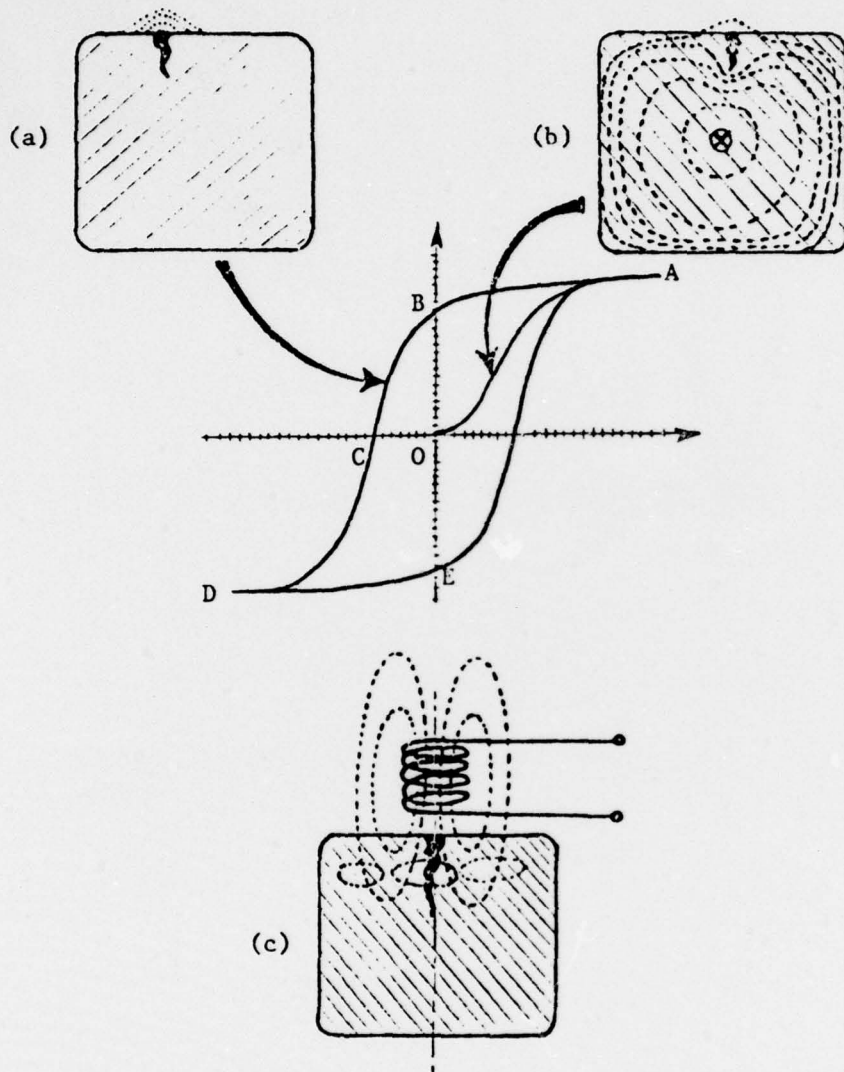
Figure 1. Electromagnetic phenomena utilized in detecting defects in ferromagnetic materials

a) Residual leakage field (region BC)
b) Active leakage field (region OA)
c) AC excitation (region ABCDEA)

electromagnetic methods of nondestructive testing, including active direct current, residual and alternating current methods of excitation.

The following sections describe:

1. Actual residual and active leakage field profiles for rectangular slots in a steel bar obtained by scanning a Hall probe over the surface of the bar.

2. Dipole model predictions for active and residual leakage fields around the same slots.

3. Finite element predictions for the active leakage fields around the same slots.

The report concludes with a discussion of the relative merits of the two modeling techniques and indicates how the finite element model might be extended to include residual magnetization and eddy current phenomena. An extensive bibliography is included for further reference.

Active and Residual Leakage Fields Around Rectangular Slots

The general shapes of residual and active leakage fields around defects in ferromagnetic materials are well known and have been widely reported in the literature[12-16]. However, in order to provide a basis of comparison with theoretical modeling studies, residual and active leakage field profiles were monitored around rectangular slots in a steel bar using the apparatus shown in Figure 2. A miniature Hall probe was used to measure the vertical component of the leakage field flux density. Leakage field profiles were obtained by driving the probe with a uniform velocity over the surface of the bar using an x-y positioning mechanism. The output of the probe was fed to a Gaussmeter having an analog output of sufficient magnitude to drive an x-y recorder.
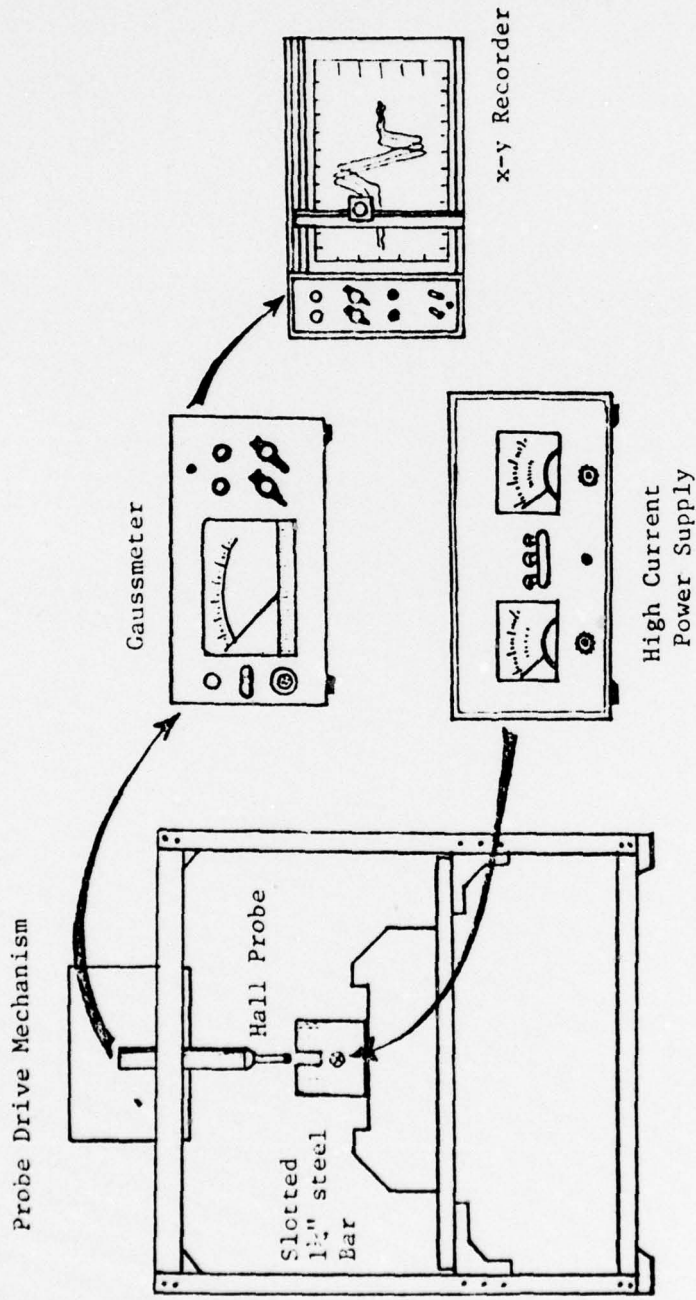
Figure 2. Experimental arrangement for the determination of residual and active leakage fields around rectangular slots in ferro-magnetic bars.
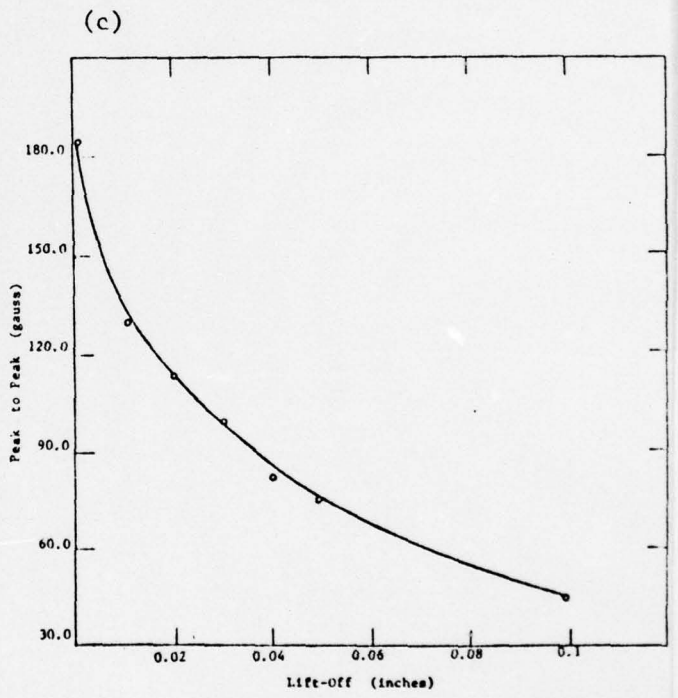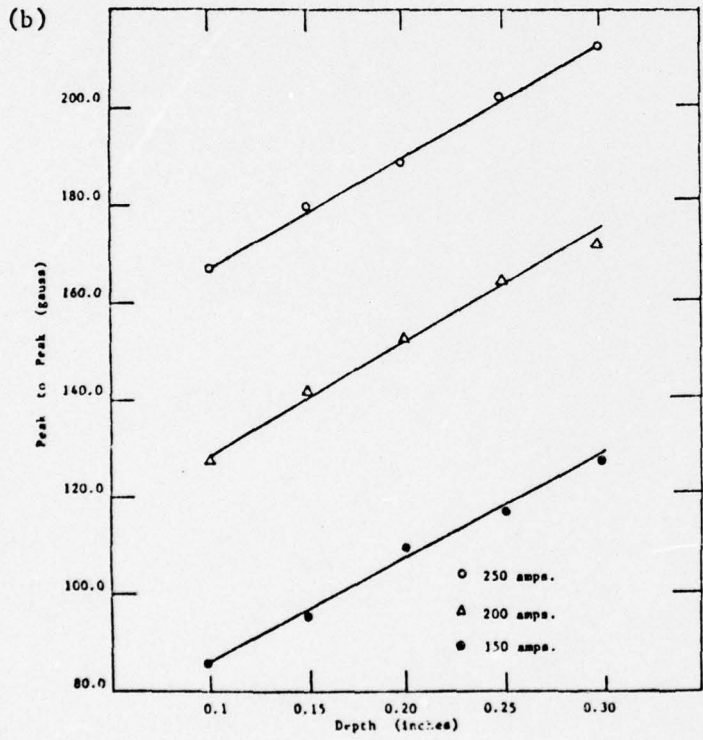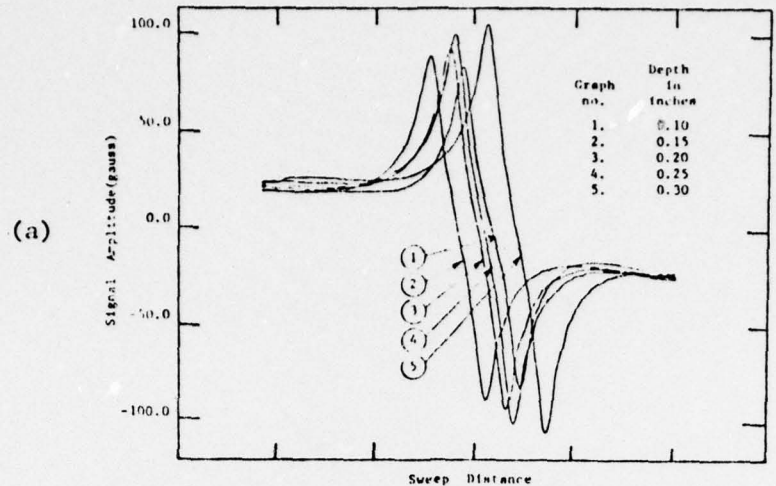
Figure 3. Active leakage field profiles for rectangular slots of constant width (0.125") and varying depth with dc excitation

a) Typical profiles
b) Peak-to-peak magnitude as a function of depth
c) A typical lift-off characteristic
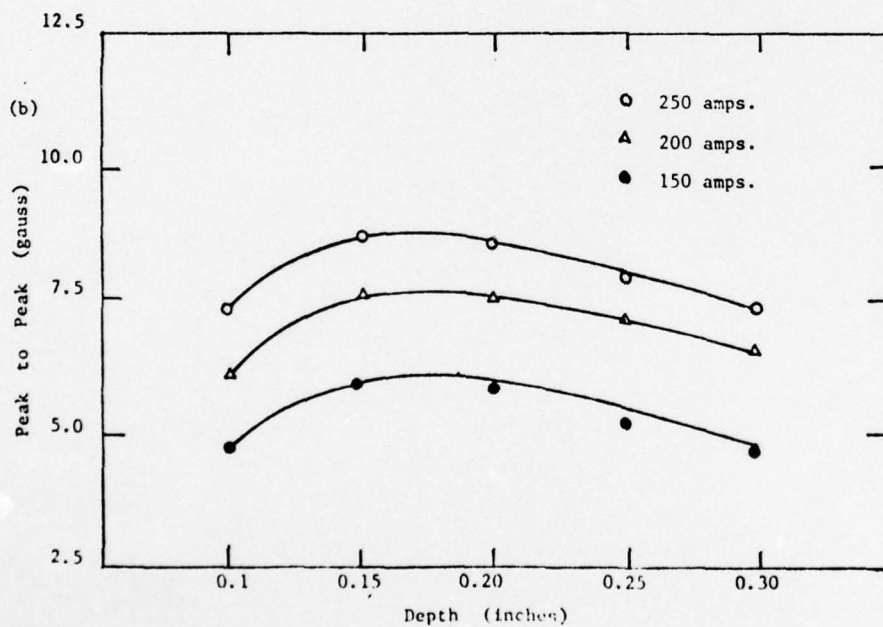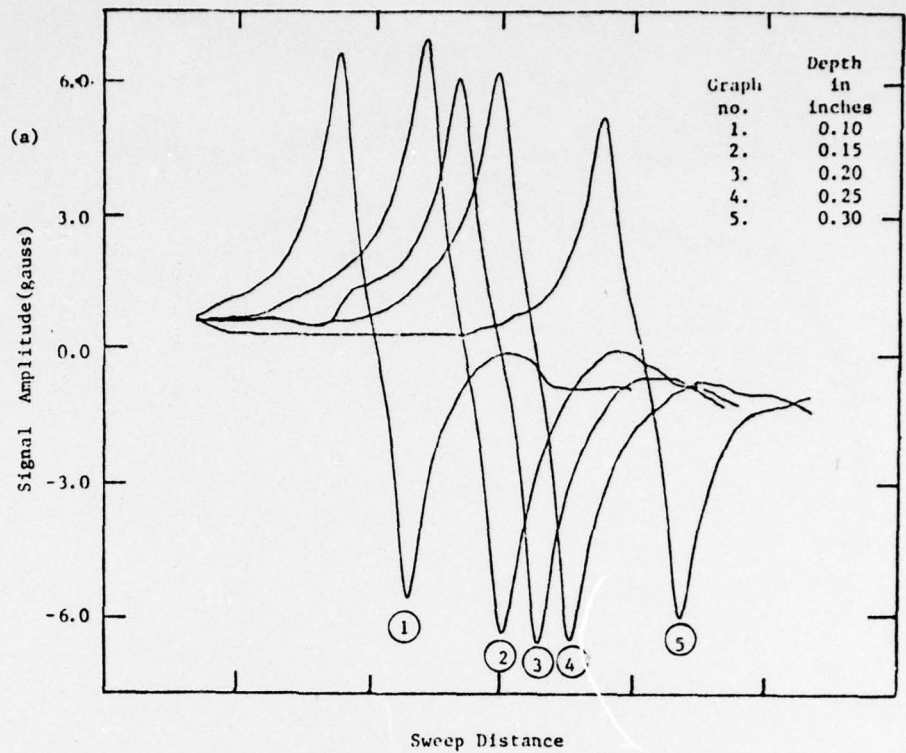
Figure 4. Residual leakage field profiles for rectangular slots of constant width (0.125") and varying depth after dc excitation

a) Typical profiles
b) Peak-to-peak magnitude as a function of depth
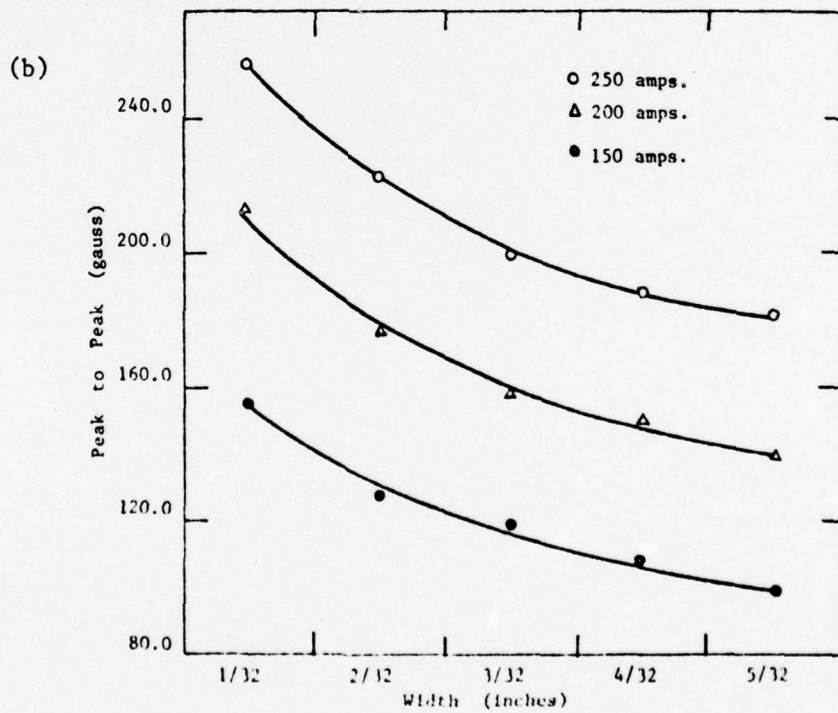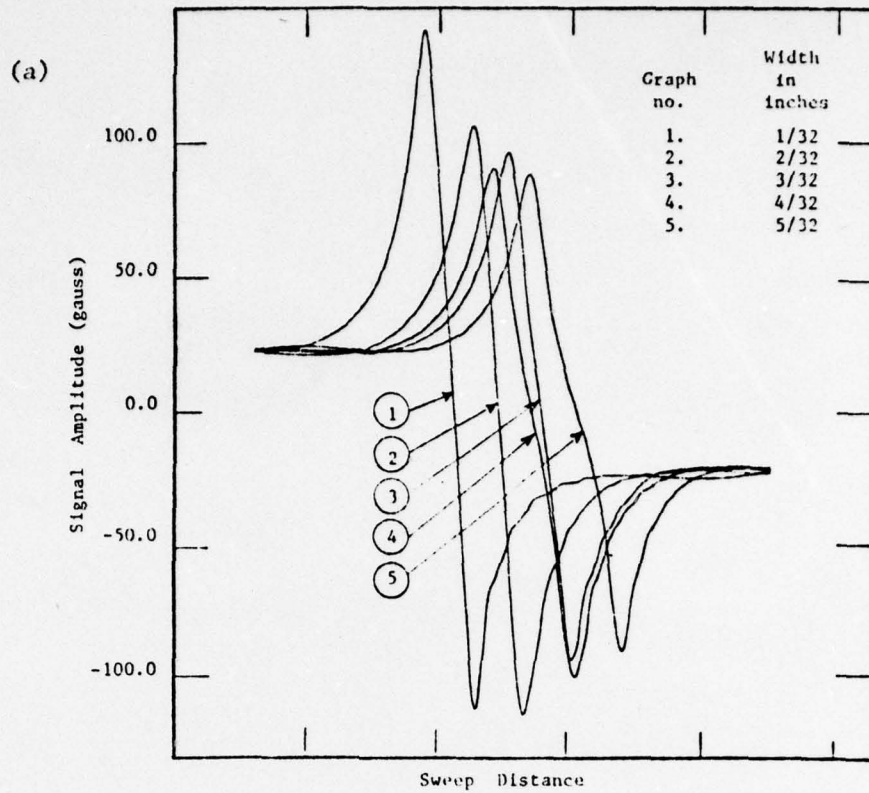
Figure 5. Active leakage field profiles for rectangular slots of
constant depth (0.2") and varying width with dc excitation

a) Typical profiles
b) Peak-to-peak magnitude as a function of width
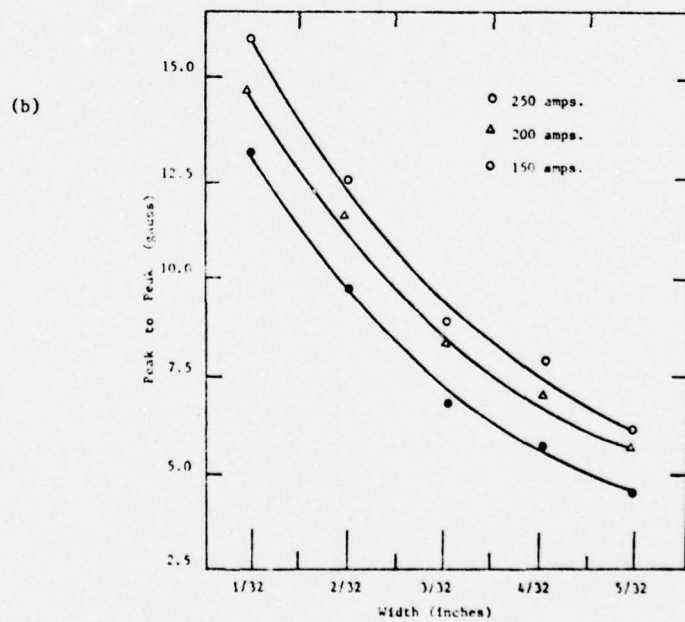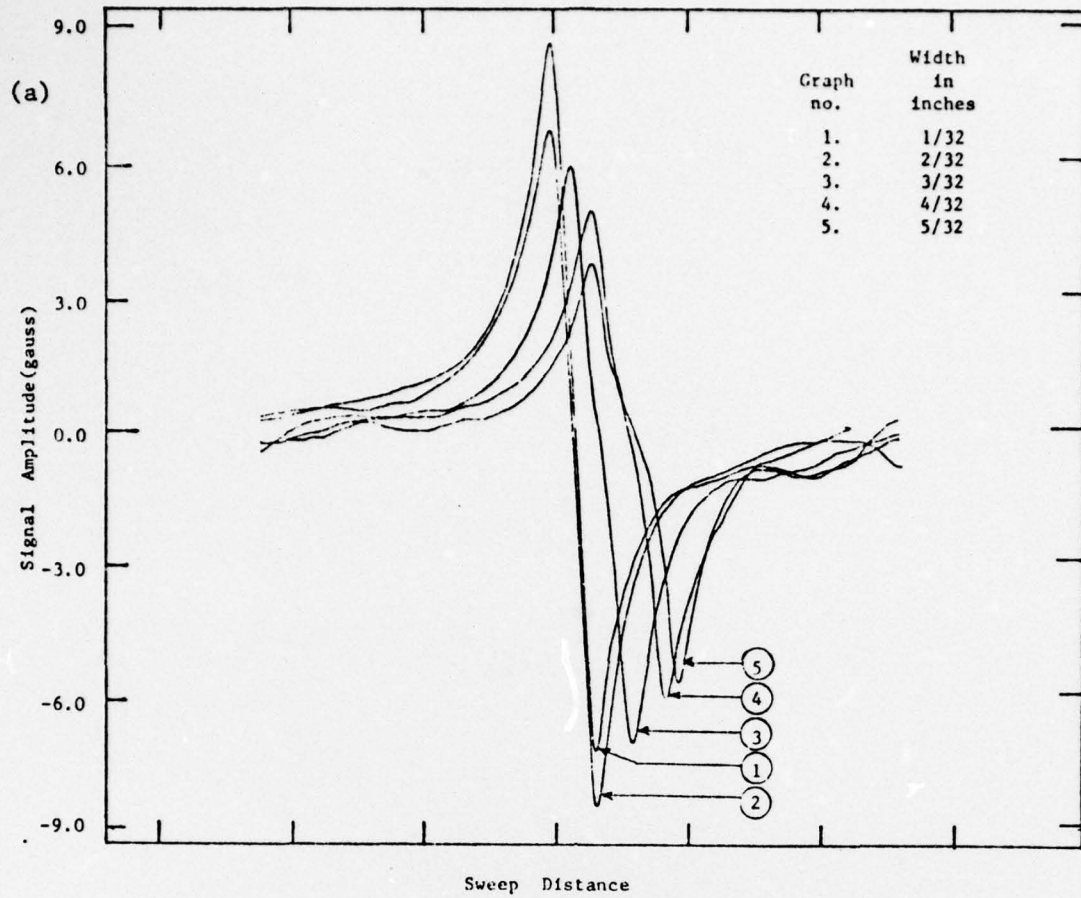
Figure 6. Residual leakage field profiles for rectangular slots of
constant depth (0.2") and varying width after dc excitation

a) Typical profiles
b) Peak-to-peak magnitude as a function of width

Typical results are shown in Figures 3, 4, 5, and 6. Both active and residual leakage field profiles for rectangular slots of constant width and varying depth are shown in Figures 3 and 4 respectively together with a typical lift-off characteristic and plots of the signals' peak-to-peak magnitudes versus depth. Corresponding results are shown in Figures 5 and 6 for rectangular slots of constant depth and varying width. Probe "lift-off" in each case was 0.015".

Note particularly the differences in peak-to-peak magnitude between the active and residual leakage fields, as well as the slight changes in profile shape.

Care was taken in setting up the experiment to ensure that a uniform magnetizing current distribution was obtained over the cross section of the specimen, and that the size of the Hall probe was sufficiently small relative to the size of the specimen that a virtual point-to-point leakage field profile was obtained by scanning over the specimen surface.

Dipole Modeling

Perhaps the most widely used model for electromagnetic field/defect interactions is that developed by Zatsepin and Shcherbinin[17]. Initially proposed for the prediction of residual leakage fields, the technique has now been improved and extended to include both dc and ac excitation conditions[18-23]. Leakage fields around rectangular slots are modeled by assuming a "uniform magnetic charge distribution" over the sides of the slot, neglecting material nonlinearities and assuming that the "charge" on the base of the slot does not contribute to the leakage field. Under these conditions expressions can be developed for the x and y components of the resulting leakage field as follows:

$$H_x = 2\sigma_s [\text{arctg} \frac{h(x+b)}{(x+b)^2 + y(y+h)} - \text{arctg} \frac{h(x-b)}{(x-b)^2 + y(y+h)}] \tag{1}$$

$$H_y = \sigma_s \ln \frac{[(x+b)^2 + (y+h)^2][(x-b)^2 + y^2]}{[(x+b)^2 + y^2][(x-b)^2 + (y+h)^2]} \tag{2}$$

where the slot width is 2b units and the slot depth is h units. σ_s is the assumed "surface charge density."

Figures 7 and 8 show plots of H_x and H_y based on equations 1 and 2 for the rectangular slots whose actual residual leakage field profiles are shown in Figures 4 and 6. The results have been normalized and a value of $\sigma_s = 1$ assumed in each case. In practice[12], σ_s values are obtained from the experimental results in order to obtain agreement between the theoretically predicted profiles and those actually measured. This has been done in Figure 9 which shows a comparison of dipole model and experimental results for a particular slot and for both residual and active magnetization conditions. In both cases the experimental peak values have been substituted into equation 2 for σ_s in order to obtain the plots.

The active magnetization case has also been included here because the dipole model, although developed initially for residual magnetization conditions[17], has also been used to model field/defect interactions with direct current excitation.

Computer code generated to produce the dipole model leakage field profiles from equations 1 and 2 is given as Appendix A. The program is self-explanatory with regard to the required input parameters and can be used to predict the leakage fields around rectangular slots. MAPA is a plotting routine available on Colorado State University's CDC 6400 computer system.
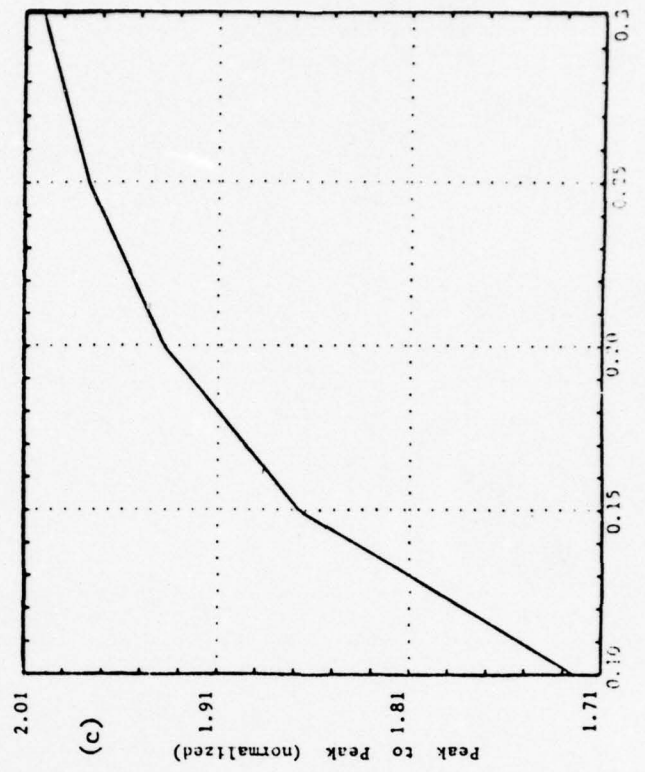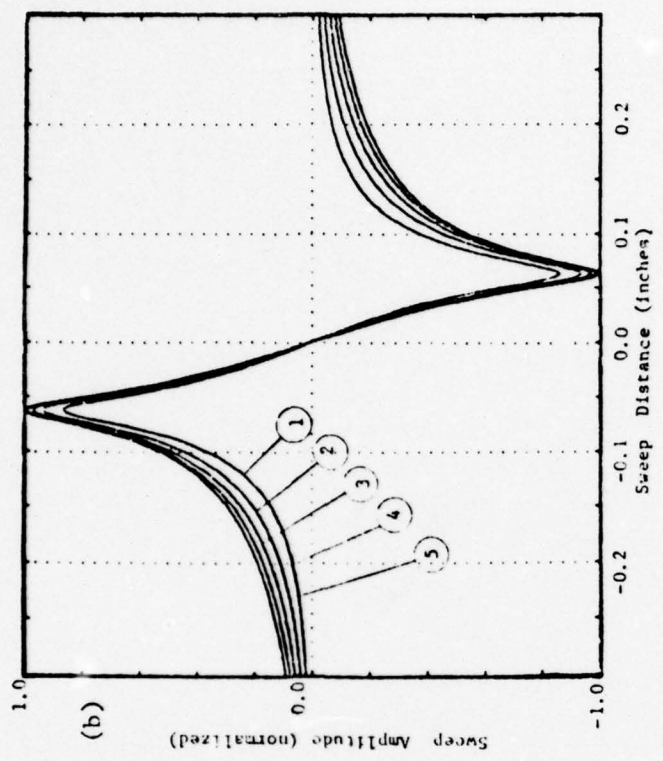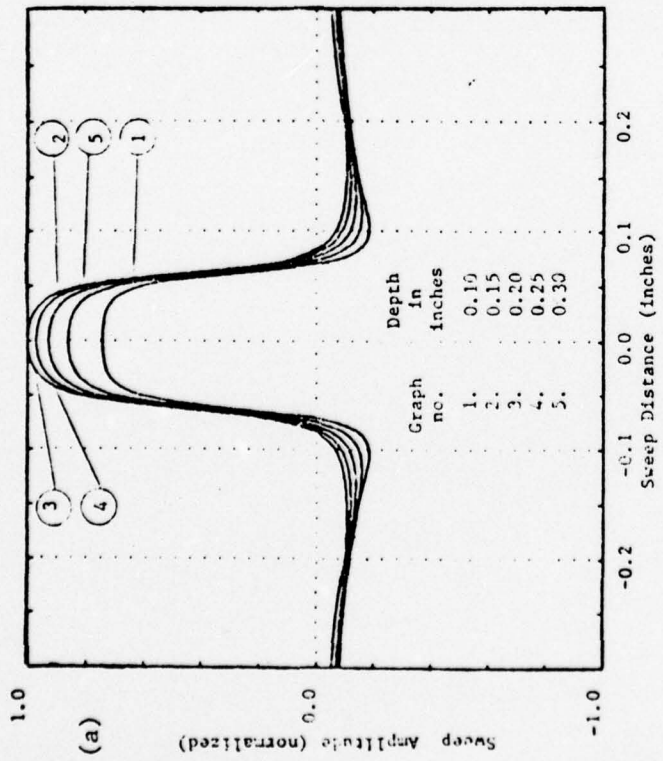
Figure 7. Leakage field profiles predicted by dipole modeling for rectangular slots of constant width (0.125") and varying depth

a) Tangential field component, H_x
b) Vertical field component, H_y
c) Peak-to-peak H_y magnitude versus depth
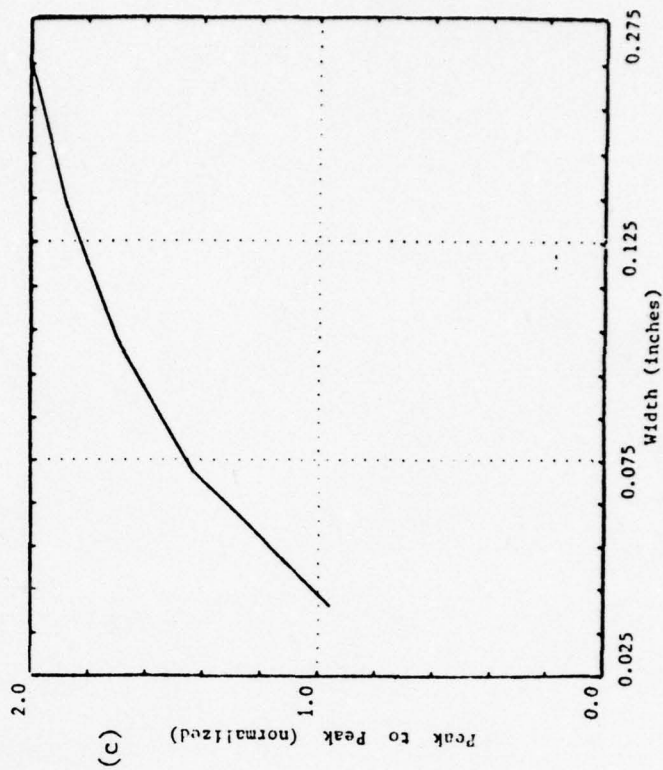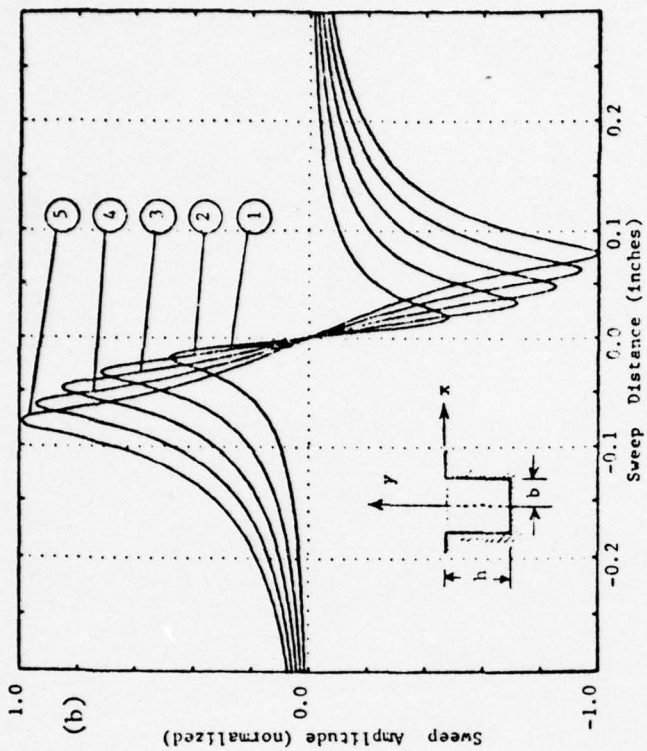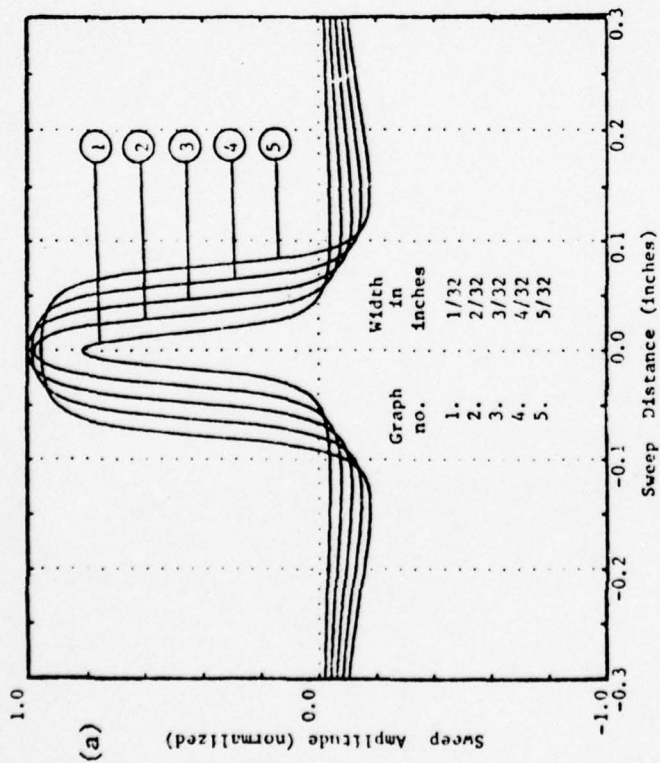
Figure 8. Leakage field profiles predicted by dipole modeling for rectangular slots of constant depth (0.2") and varying width

a) Tangential field component, H_x
b) Vertical field component, H_y
c) Peak-to-peak H_y magnitude versus width
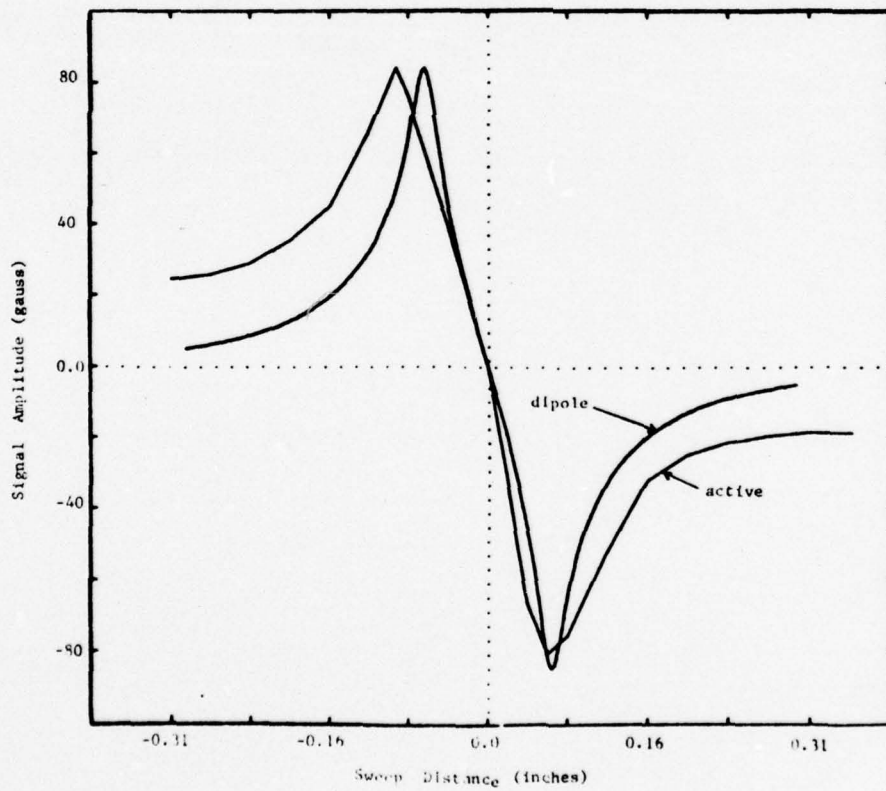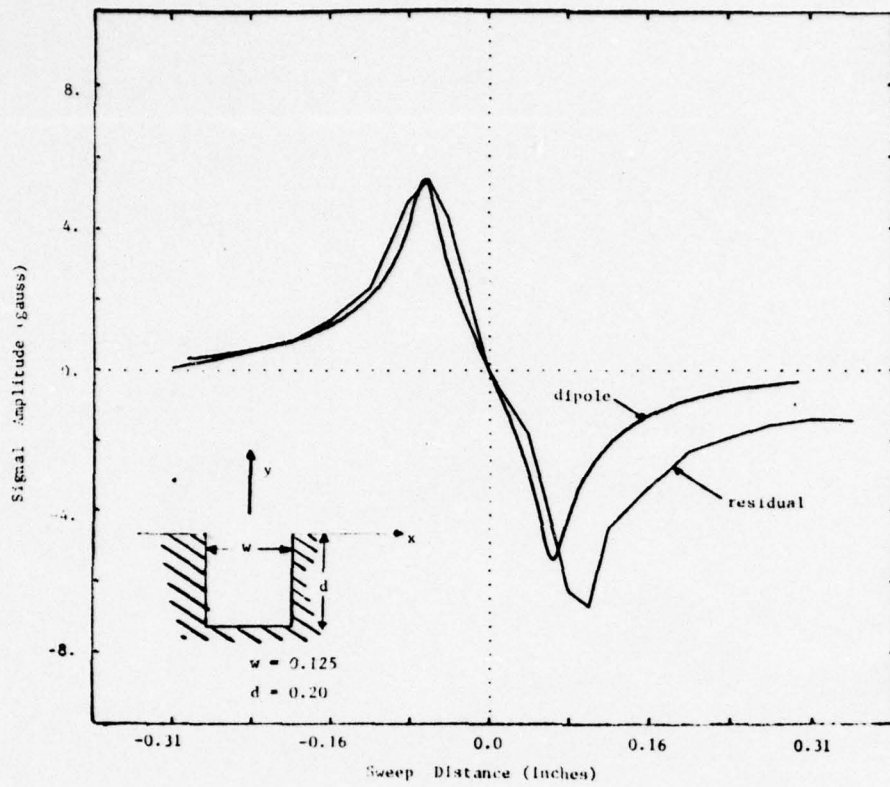
Figure 9. Comparison of dipole model predictions and experimental results for the (0.125" x 0.2") slot.

a) Residual leakage field profiles after 250 amps excitation.

b) Active leakage field profiles with 250 amps excitation.

Finite Element Modeling

Although considerable work has been done to develop closed form mathematical solutions for the prediction of leakage fields around defects in the case of dc[24] and ac[25,26] excitation conditions, the results do not lend themselves well to the general approach to defect characterization called for in the introduction. The primary reason for this is that, although the equations governing the electromagnetic field/defect interactions are readily obtainable in a poissonian partial differential equation form, the nonlinear magnetization characteristics of ferromagnetic materials and complex defect geometrics found in practice prevent closed form solutions from being obtained for anything but the simplest conditions.

Developments in numerical analysis technqiues have had a significant impact on the study of magnetic flux distributions in electrical machinery[27-31] and the principal investigator strongly suggests that such analysis techniques could have a similar impact on the problem of defect characterization schemes for electromagnetic methods of nondestructive testing. In the case of a ferromagnetic bar carrying a dc magnetization current the vector potential, A in the region is related to the current density, J and reluctivity (H/B), ν by the equation

$$\frac{\partial}{\partial x}\left(\nu\frac{\partial A}{\partial x}\right) + \frac{\partial}{\partial y}\left(\nu\frac{\partial A}{\partial y}\right) = -J \tag{3}$$

assuming that the bar is at the center of an unconventional coordinate axis system and carrying current in the positive z direction. The finite element analysis approach to solving equation 3 is based on:

1. Discretizing the region of interest, R, into triangular elements.
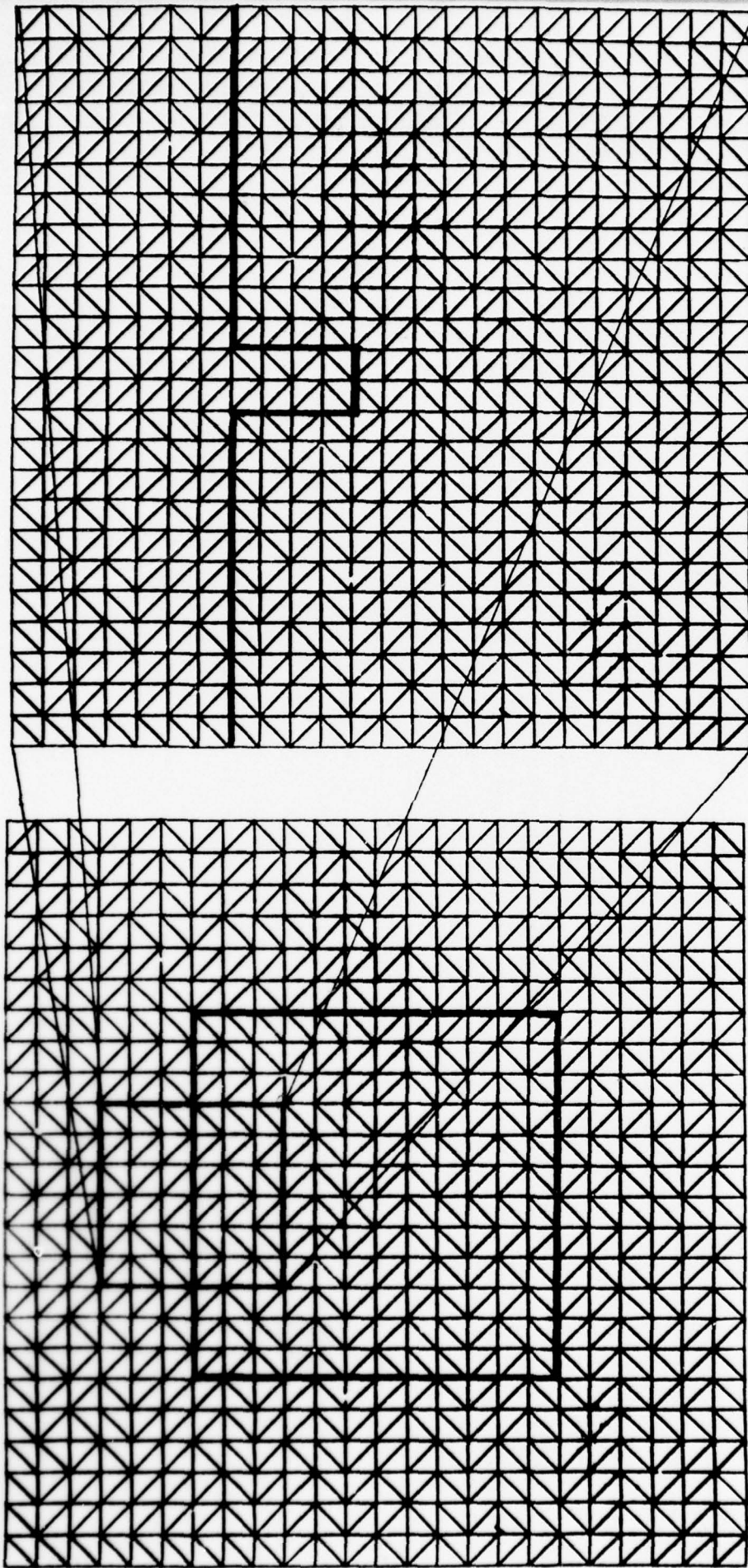
Figure 10. Mesh generation for the finite element modeling of leakage fields around rectangular slots in a ferromagnetic bar.

a) Gross mesh.

b) "Zoom-in" region.
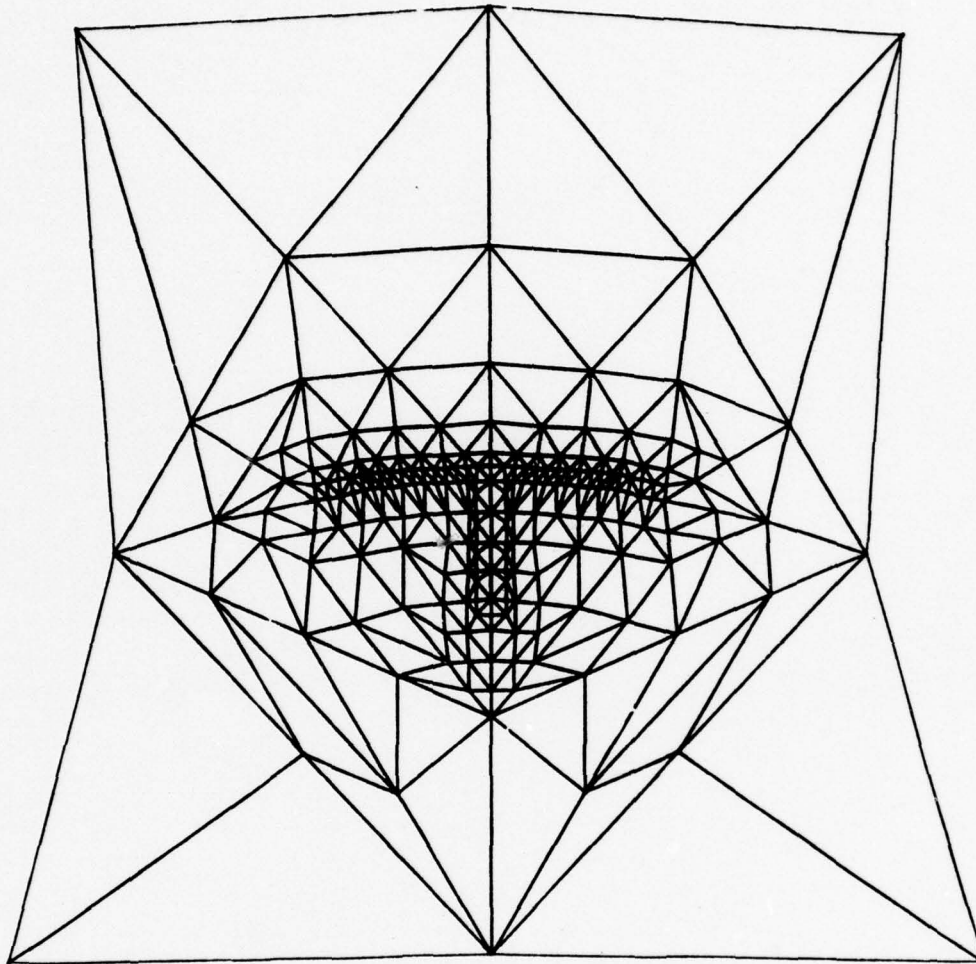
Figure 11. Hand generated mesh for detailed study of leakage fields around small slots[38].

2. Minimizing an energy functional, in this case

$$W = \iint_R [\int_o^B \nu b \, db] dx \, dy - \iint_R JA \, dx \, dy \tag{4}$$

over the discretized region to yield a set of equations for the vector potential at each node of the form

$$A_{node} = f(J, \nu, A_{adjacent\ nodes}, x, y) \tag{5}$$

3. Solving the nodal vector potential equations by matrix inversion or iterative techniques.

The finite element code given as Appendix B is based directly on Anderson's method[32]. Discussions of energy functionals, convergence, mesh subdivision and B/H curve modeling can be found in references 33 to 37. The code is self explanatory with regard to the required input data and consists of three distinct parts:

1. Mesh generation algorithm (B.1)

2. Element ordering algorithm (B.2)

3. Vector potential and flux density calculation algorithm (B.3)

This format allows maximum flexibility to examine a wide variety of geometries although the three parts could be run together if needed.

In examining the leakage field around relatively small slots in the surface of a square ferromagnetic bar it is possible to "zoom in" on the region of interest by making two runs with the computer code. First, a mesh is generated as in Figure 10a) for the square bar and a surrounding air region of sufficient size that the vector potential, A, is zero on the outer boundary. The boundary can be found experimentally, using a gaussmeter, or by a trial-and-error approach, applying the computer code several times until no further change in A is observed

with changes in outer boundary position. After calculating the vector
potential at every node within this mesh, the "zoom in" region around
the defect is chosen, as shown in Figure 10b), with the vector potentials
on the region perimeter serving as boundary conditions for the second run.
Some form of linear interpolation must be used to find all nodal A values
for this second run, or a hand-generated mesh could be used similar to
the one shown in Figure 11. This technique was used by Hwang and Lord
for a variety of defect shapes and, based on the results, a defect
characterization scheme was proposed for electromagnetic methods of
nondestructive testing relying on active dc magnetization conditions[38-40].
The results shown in Figure 13 were obtained using the mesh of Figure 12
and the computer program listed as Appendix B.3.

Discussion

In order to develop defect characterization schemes for electro-
magnetic methods of nondestructive testing, a flexible mathematical
model is needed to predict magnetic field/defect interactions under the
constraints of nonlinear operating conditions and awkward boundary
shapes. Although the dipole model predicts the shape of leakage field
profiles around rectangular slots in ferromagnetic materials, the under-
lying linearizing assumptions associated with the technique prevent
its use as the basis for defect characterization schemes.

Finite element analysis techniques have been applied with success
to the prediction of magnetic fields in electrical machines and this
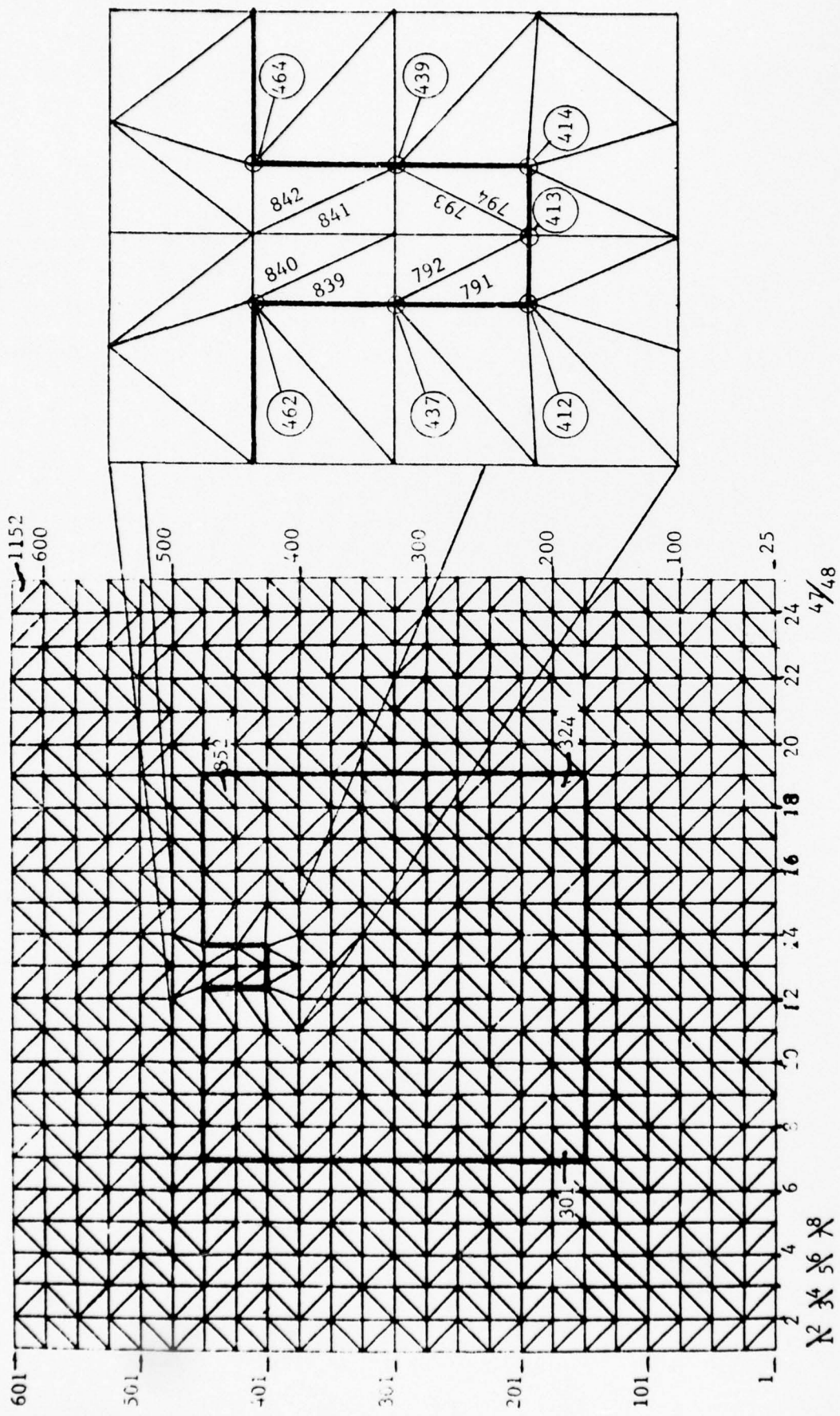
Figure 12. Modified computer generated mesh for results of Figure 13. Inset shows slot node numbering detail.
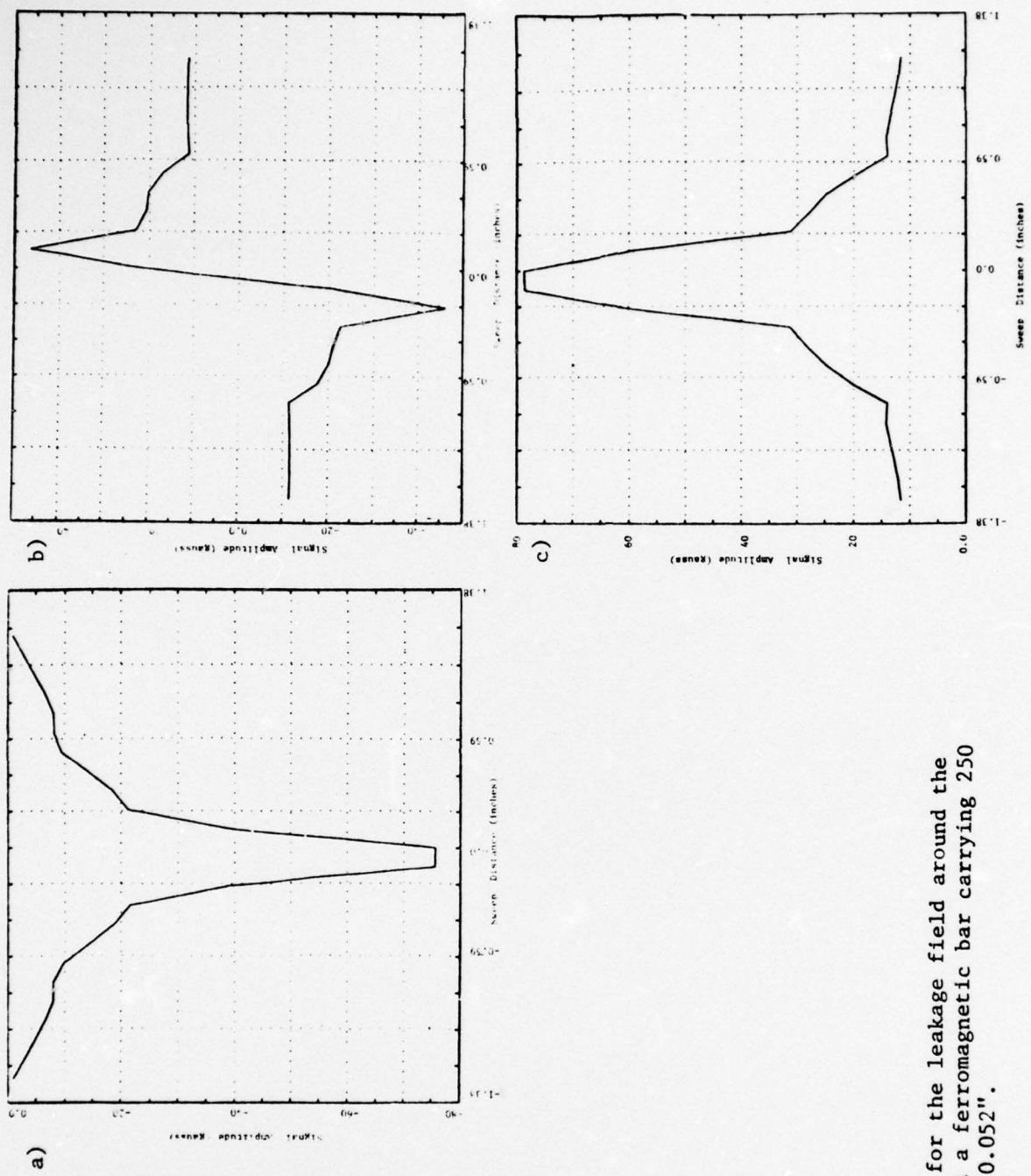
Figure 13.

Finite element results for the leakage field around the (0.125" x 0.2") slot in a ferromagnetic bar carrying 250 amps. Probe lift-off = 0.052".

a) B_x component.
b) B_y (normal) component.
c) $B = (B_x^2 + B_y^2)^{\frac{1}{2}}$.

technical report shows how they can be used to predict leakage fields around slots in ferromagnetic materials excited with a dc magnetization current. Certain assumptions do have to be made with regard to the location of the zero vector potential boundary, discretization and B/H curve model, but on the whole, finite element techniques are sufficiently flexible and accurate to be applied to the defect characterization or "inverse" problem.

With regard to extending the techniques to other forms of excitation, the following comments are offered:

Residual leakage fields exist around defects in ferromagnetic materials after initial magnetization with a dc current, causing regions around the defect to behave as permanent magnets working in the second quadrant of the material's B-H loop represented by region BC in Figure 1. Some work has been done in studying flux distributions in permanent magnet machines using numerical analysis techniques[41-44] which could be applied to the modeling of leakage field profiles. Experimental studies of the residual fields within slots in ferromagnetic materials are being carried out by the authors at Colorado State University to define in detail the permanent magnet behavior of the material in the vicinity of the slot. The results will provide needed modeling data for the finite element program which in this case provides an approximate solution for the equation

$$\frac{\partial}{\partial x} (\nu \frac{\partial A}{\partial x}) + \frac{\partial}{\partial y} (\nu \frac{\partial A}{\partial y}) = J_m \tag{6}$$

where J_m is similar to the current density term of equation 3, but in this case models the behavior of the permanent magnet material[43].

Eddy currents and their associated fields set up by an ac excitation current, react with a defect to produce an effective change in the impedance of a pick-up coil scanning above the surface of the material under test. In this case the material in the vicinity of the defect is cycled through a complete B-H loop (ABCDEA in Figure 1) and the governing equation to be solved by numerical techniques is of the form

$$\frac{\partial}{\partial x}\left(\nu\frac{\partial A}{\partial x}\right) + \frac{\partial}{\partial y}\left(\nu\frac{\partial A}{\partial y}\right) = i\sigma\omega A - J_s \tag{7}$$

where J_s is the imposed current density, ω is the angular frequency and σ the conductivity of the material. This type of equation has recently been solved for electrical machine applications[45-50] using finite difference and finite element analysis and such techniques could also be used to study basic eddy current phenomena associated with electromagnetic methods of nondestructive testing.

Although equations 3, 6 and 7 are given in two dimensional form, recent work[51,52] would indicate that three dimensional solutions may be available in the future.

References

1. Bray, D. E. "Railroad Accidents and Nondestructive Inspection." Presented at the ASME Winter Annual Meeting, Paper No. 74-WA/RT-4, November 17, 1974.

2. Darcy, G. "Economic Motivation and Potential Impact of NDE in DOD, Proceedings of the Interdisciplinary Workshop for Quantitative Flaw Definition." AFML publication TR-74-238, June 1974, pp. 68-84.

3. Knight, S. R. "NDT for Nuclear Power." Materials Evaluation, May 1973, pp. 19-24.

4. Dau, G. J. "Rationale for Inservice Inspection During Nuclear Power Plant Design/Fabrication." Presented at the American Nuclear Society 23rd Annual Meeting, New York, June 1977.

5. Thompson, R. B. "Overview of the ARPA/AFML Program for Quantitative Flaw Definition." Proceedings of the ARPA/AFML Review of Progress in Quantitative NDE, AFML publication TR-77-44, September 1977, pp. 109-115. (Several papers relating to this work appeared in the first edition of the quarterly Research Supplement to Materials Evaluation, April 1977).

6. Adler, L. and Lewis, D. K. "Models for the Frequency Dependence of Ultrasonic Scattering from Real Flaws." ibid., pp. 180-186

7. Krumhansl, J. A. "Interpretation of Ultrasonic Scattering Measurements by Various Flaws from Theoretical Studies." ibid., pp. 164-172

8. Mucciardi, A. N. "Adaptive Nonlinear Modeling for Ultrasonic Signal Processing," Proceedings of the Interdisciplinary Workshop for Quantitative Flaw Definition. AFML publication TR-74-238, June 1974, pp. 194-212.

9. Stumm, W. "Multiparameter-Methoden in der zerstörungsfreien Werkstoffprüfung," Materialprüfung. Vol. 19, April 1977, pp. 131-136.

10. Sukhorukov, V. V., Ullitin, Y. M., Chernov, L. A. "Feasibility of Determining Defect Parameters by Eddy Current Modulation Defectoscopy," Defektoskopiya. No. 1, January-February, 1977, pp. 7-14.

11. Lord, W. and Oswald, D. J. "Leakage Field Methods of Defect Detection," International Journal of NDT. Vol. 4, 1972, pp. 249-274.

12. Shcherbinin, V. E., and Zatsepin, N. N. "Calculation of the Magnetostatic Field of Surface Defects, II. Experimental Verification of the Principal Theoretical Relationships." Defektoskopiya, No. 5, September-October, 1966, pp. 59-65.

13. Lankford, J., and Francis, P. H. "Magnetic Field Perturbation Due to Metallurgical Defects." International Journal of Nondestructive Testing, Vol. 3, 1971, pp. 77-94.

14. Lord, W., and Oswald, D. J. "The Generated Reaction Field Method of Detecting Defects in Steel Bars." Materials Evaluation, Vol. 29, No. 2, February 1971, pp. 21-28.

15. Vlasov, V. V. and Volkov, B. I. "Applied Eddy Current System Having a Hall Plate as the Searcher and Reacting to the Tangential Component of the Defect Field." Defektoskopiya, No. 1, January-February, 1977, pp. 84-90.

16. Shiraiwa, T., et. al. "An Automatic Magnetic Inspection Method Using Magnetoresistive Elements and its Application." Materials Evaluation, May 1973, pp. 90-96.

17. Zatsepin, N. N. and Shcherbinin, V. E. "Calculation of the Magneto-static Field of Surface Defects. I. Field Topography of Defect Models." Defektoskopiya, No. 5, October 1966, pp. 50-59.

18. Shcherbinin, V. E., and Pashagin, A. I. "Influence of the Extension of a Defect on the Magnitude of its Magnetic Field." Defektoskopiya, No. 4, July-August 1972, pp. 74-82.

19. Novikova, I. A., and Miroshin, N. V. "Investigation of the Fields of Artificial Open Flaws in a Uniform Constant Magnetic Field." Defektoskopiya, No. 4, July-August 1973, pp. 95-101.

20. Burtsev, G. A., and Fedorishcheva, E. E. "Simple Approximation for the Magnetostatic Fields of Surface Defects and Inhomogeneities." Defektoskopiya, No. 2, March-April 1974, pp. 111-119.

21. Shcherbinin, V. E., and Pashagin, A. I. "Polarization of Cracks in Nonuniformly Magnetized Parts." Defektoskopiya, No. 3, May-June 1974, pp. 17-23.

22. Shcherbinin, V. E., and Pashagin, A. I. "On the Volume Polarization of Cracks." Defektoskopiya, No. 4, July-August 1974, pp. 106-110.

23. Domashevskii, B. N., and Geiser, A. I. "Polarization of Cracks when Magnetized in a Longitudinal Alternating Field." Defektoskopiya, No. 2, March-April 1976, pp. 89-95.

24. Kolodii, B. I., and Teterko, A. Y. "Determination of the Transverse Magnetostatic Field of a Cylinder with an Eccentric Cylindrical Inclusion." Defektoskopiya, No. 3, May-June 1976, pp. 44-51.

25. Burrows, M. "Theory of Eddy-Current Flaw Detection." Ph.D. Thesis, University of Michigan, University Microfilms, Inc., Ann Arbor, Michigan.

26. Dodd, C. V., et. al. "Some Eddy Current Problems and their Integral Solutions." Oak Ridge National Laboratory Report 4384, Contract No. W-7405-eng-26, Oak Ridge, Tennessee, April 1969.

27. Winslow, M. A. "Numerical Solution of the Quasilinear Poisson Equation in a Nonuniform Triangle Mesh." Journal of Computational Physics, Vol. 2, 1967, pp. 149-172.

28. Erdelyi, E. A., et. al. "Nonlinear Magnetic Field Analysis of dc Machines." IEEE Transactions on Power Apparatus and Systems, Vol. 89, 1970, pp. 1546-1583.

29. Chari, M. V. K., and Silvester, P. "Finite Element Analysis of Magnetically Saturated dc Machines." IEEE Transactions on Power Apparatus and Systems, Vol. 90, 1971, pp. 2362-2372.

30. Anderson, O. W. "Transformer Leakage Flux Program Based on the Finite Element Method." IEEE Transactions on Power Apparatus and Systems, Vol. 92, 1973, pp. 682-689.

31. Lord, W., and Hwang, J. H. "Leakage Field Analysis of Magnetic Circuits by Variational Methods." Proceedings of the Fourth Annual Symposium on Incremental Motion Control Systems and Devices, University of Illinois, April 1975, pp. P1-P9.

32. Anderson, O. W. "Iterative Solution of Finite Element Equations in Magnetic Field Problems." Conference paper C72 425-7, IEE PES Summer Meeting, San Francisco, July, 1972.

33. Brauer, J. R. "Saturated Magnetic Energy Functional for Finite Element Analysis of Electric Machines." Conference paper C75 151-6, IEEE PES Winter Meeting, New York, January 1975.

34. Carol, B. A. "The Determination of the Optimum Acceleration Factor for Successive Over-relaxation." Computer Journal, Vol. 4, 1961, pp. 73-78.

35. Lord, W., and Hwang, J. H. "Convergence and Mesh Subdivision for Finite Element Analysis of Non-linear Magnetic Fields." International Journal of Computers and Electrical Engineering, Vol. 1, No. 4, 1974, pp. 513-520.

36. Fischer, J., and Moser, H. "Die Nachbildung von Magnetisierungskurven durch einfache algebraische oder transzendente Funktionen." Archiv für Elektrotechnik, Vol. 42, No. 5, 1956, pp. 286-299.

37. Trutt, F. C., et al. "Representation of the Magnetization Characteristic of dc Machines for Computer Use." IEEE Transactions on Power Apparatus and Systems, Vol. 87, March 1968, pp. 665-669.

38. Lord, W., and Hwang, J. H. "Finite Element Modeling of Magnetic Field/Defect Interactions." ASTM Journal of Testing and Evaluation, Vol. 3, No. 1, January 1975, pp. 21-25.

39. Hwang, J. H., and Lord, W. "Magnetic Leakage Field Signatures of Material Discontinuities." Proceedings of the Tenth Symposium on Nondestructive Evaluation, San Antonio, April 1975, pp. 63-76.

40. Lord, W., and Hwang, J. H. "Defect Characterization from Magnetic Leakage Fields." British Journal of Nondestructive Testing, Vol. 19, No. 1, January 1977, pp. 14-18.

41. Reichert, K. "The Calculation of Magnetic Circuits with Permanent Magnets by Digital Computers." IEEE Transactions on Magnetics, Vol. 6, No. 2, June 1970.

42. Kamminga, W. "Finite Element Solutions for Devices with Permanent Magnets." Journal of Physics D: Applied Physics, Vol. 8, 1975, pp. 841-855.

43. Binns, H. J., et. al. "Computation of the Magnetic Field of Permanent Magnets in Iron Cores." Proceedings IEE, Vol. 122, No. 12, December 1975, pp. 1377-1381.

44. Lord, W. "Permanent Magnet Modelling for Machine Applications." COMPUMAG Proceedings, Rutherford Laboratory, Oxford, 1976, pp. 198-204.

45. Chari, M. V. K. "Finite Element Solution of the Eddy Current Problem in Magnetic Structures." IEEE Transactions on Power Apparatus and Systems, Vol. 93, No. 1, January-February 1974, pp. 62-72.

46. Stoll, R. L. "The Analysis of Eddy Currents." Clarendon Press, Oxford, 1974.

47. Sato, T., et. al. "Calculation of Magnetic Field Taking into Account Eddy Current and Nonlinear Magnetism." Electrical Engineering in Japan, Vol. 96, No. 4, 1976, pp. 96-102.

48. Brauer, J. R. "Finite Element Analysis of Electromagnetic Induction in Transformers." Presented at the IEEE Winter Power Meeting, New York, January 1977.

49. Anderson, O. W. "Finite Element Solution of Skin Effect and Eddy Current Problems." Presented at the IEEE PES Summer Meeting, Mexico City, July 1977.

50. Chari, M. V. K., and Csendes, Z. J. "Finite Element Analysis of the Skin Effect in Current Carrying Conductors." IEEE Transactions on Magnetics, Vol. 13, No. 5, September 1977, pp. 1125-1127.

51. Guancial, E., and DasGupta, S. "Three Dimensional Finite Element Program for Magnetic Field Problems." IEEE Transactions on Magnetics, Vol. 13, No. 3, May 1977, pp. 1012-1015.

52. Zienkiewicz, O. C., et. al. "Three Dimensional Magnetic Field Determination Using a Scalar Potential - A Finite Element Solution." IEEE Transactions on Magnetics, Vol. 13, No. 5, September 1977, pp. 1649-1656.

Appendix A

Dipole modeling code for rectangular slots.

```
1          PROGRAM DIPOL3
           1 (INPUT,OUTPUT,TAPE5=INPUT,TAPE6=OUTPUT,FILMPL)
   C
   C
   C
   C        **********                                      **********
   C
   C        PROGRAM DIPOL3 CALCULATES THE MAGNETIC FIELD AROUND A RECTANGULAR
   C        DEFECT, USING A STRIP DIPOLE MODEL.
   C
   C        THE REQUIRED INPUT CONSISTS OF THE FOLLOWING DATA.
   C        .....(SIGMA) IS A SCALING CONSTANT USED TO DESCRIBE THE LINEAR
   C             DENSITY OF THE MAGNETIC CHARGE ALONG THE SURFACE OF THE
   C             DEFECT.
   C        .....(Y) DESCRIBES THE LIFT-OFF IN INCREMENTS OF (INCR).
   C        .....(IDATA) SPECIFIES THE TOTAL NUMBER OF DEFECTS EXAMINED.
   C        .....(MIN) AND (MAX) ARE THE MINIMUM AND MAXIMUM POINTS TO BE
   C             SPECIFIED TO EITHER SIDE OF THE CENTER OF THE DEFECT.  THE
   C             SPACING BETWEEN POINTS IS (INCRX).
   C        .....(H1) AND (W) ARE THE DEPTH AND WIDTH MEASUREMENTS OF THE
   C             DEFECT (IN UNITS OF (INCR)).
   C        .....A CROSS-SECTION OF THE RECTANGULAR SLOT IS SHOWN BELOW.
   C
   C                                     W
   C               **********         **********
   C                        *         *
   C                        *         *
   C                        *         * H1
   C                        *         *
   C                        *         *
   C                        *************
   C
   C
   C        THE OUTPUT INCLUDES THE MAXIMUM VALUES FOUND FOR THE MAGNETIC
   C        FIELD IN BOTH THE X AND Y DIRECTIONS ((BX) AND (BY),RESPECTIVELY),
   C        THE VALUES USED FOR (SIGMA), (MIN), (MAX), (Y), AND (INCR), AND
   C        THE PER UNIT VALUES USED FOR EACH DEFECT.  THIS PROGRAM ALSO
   C        PRODUCES MICROFILM PLOTS OF THE MAGNETIC FIELD VALUES (BX), (BY),
   C        AND (BT) AT A SPECIFIED LIFT-OFF.  (BT) IN THIS CASE IS THE TOTAL
   C        MAGNETIC FIELD, DEFINED AS
   C                    BT=(BX**2+BY**2)**0.5.
   C        PLOTS OF PEAK TO PEAK (BY) VALUES VERSUS DEFECT DEPTH AND WIDTH
   C        ARE SHOWN NEXT, ACCOMPANIED BY TABLES LISTING THE VALUES USED IN
   C        ALL THE PLOTS.
   C
   C        **********                                      **********
   C
   C
   C
   C
           DIMENSION
          1 HX(5,241),HY(5,241),HXY(5,241),XX(241)
          2 ,H1(5),H(5),W(5),B(5)
          3 ,H2(241),H3(241),H4(241),H5(241),H9(241)
          4 ,HY4(5),HY5(5),XY1(5),XY2(5)
          * ,MTIT(8),MTI2(8),MTI3(8)
           REAL INCR ,INCRX
           INTEGER XT(8),YT(8),XXT(8),YTT(8),XTT(8)
           DATA
          1 XT/10HX DIST(IN),7*1H /,YT/8*1H /,XXT/10HDEPTH     ,7*1H /
          2 ,YTT/10HP-P       ,7*1H /,YTT/10HWIDTH     ,7*1H /
```

```
C
C-----DATA INPUT
C
      READ(5,100) SIGMA
      READ (5,101) Y,INCR,INCRX
      READ (5,102) IDATA,MIN,MAX
      READ (5,103) (H1(I),W(I),I=1,IDATA)
C
C-----INITIALIZATION OF VARIABLES
C
      HY3=0.0
      HX3=0.0
      MA=-MIN+MAX+1
      N=0
      Y=Y*INCR
      DO 200 I=1,IDATA
      HY4(I)=0.0
      HY5(I)=0.0
      H(I)=0.0
      B(I)=0.0
 200  CONTINUE
C
C-----CALCULATATION OF BX AND BY
C
      DO 250 I=1,IDATA
       H(I)=H1(I)*INCR
       B(I)=(W(I)/2)*INCR
      DO 250 M=1,MA
        XX(M)=(FLOAT(M-1+MIN)*INCRX)
C
        X1=XX(M)
      D1=((X1+B(I))**2)+(Y*(Y+H(I)))
      D2=((X1-B(I))**2)+(Y*(Y+H(I)))
      HX1=ATAN((H(I)*(X1+B(I)))/D1)
      HX2=ATAN((H(I)*(X1-B(I)))/D2)
      HX(I,M)=2*SIGMA*(HX1-HX2)
C
        IF(HX(I,M).GE.HX3.AND.HX(I,M).GT.0.0) HX3=HX(I,M)
C
      D3=((X1+B(I))**2+(Y+H(I))**2)*((X1-B(I))**2+Y**2)
      D4=((X1+B(I))**2+Y**2)*((X1-B(I))**2+(Y+H(I))**2)
      HY(I,M)=SIGMA*ALOG(D3/D4)
C
        IF(HY(I,M).GE.HY3.AND.HY(I,M).GT.0.0) HY3=HY(I,M)
        IF (HY(I,M).LE.HY4(I).OR .HY(I,M).LT.0.0) GO TO 230
        HY4(I)=HY(I,M)
        XY1(I)=X1
        GO TO 240
 230    CONTINUE
        IF(HY(I,M).GE.HY5(I).OR .HY(I,M).GT.0.0) GO TO 240
        HY5(I)=HY(I,M)
        XY2(I)=X1
 240    CONTINUE
 250  CONTINUE
```

```
C
C------CALCULATION OF UNIT VALUES
C
      DO 260 I=1,IDATA
      XMAX=ABS(HX3)
      YMAX=ABS(HY3)
       HY4(I)=HY4(I)/YMAX
       HY5(I)=HY5(I)/YMAX
      DO 260 J=1,MA
        HX(I,J)=HX(I,J)/XMAX
        HY(I,J)=HY(I,J)/YMAX
        HXY(I,J)=SQRT((HX(I,J))**2+(HY(I,J))**2)
 260  CONTINUE
C
C------PRINT OUTPUT
C
      WRITE(6,110)HX3,HY3
      WRITE (6,112) SIGMA,MIN,MAX
      WRITE (6,113) Y
      WRITE (6,114) INCR
      DO 270 J=1,IDATA
      WRITE (6,111) J,IDATA
      WRITE (6,115) W(J)
      WRITE (6,116) H1(J)
 270  CONTINUE
C
C------PLOTS AND DATA
C
 267  DO 300 J=1,IDATA
      DO 300 M=1,MA
      GO TO (277,278,279,280, 284),J
 277  H2(M)=HX(J,M)
      GO TO 300
 278  H3(M)=HX(J,M)
      GO TO 300
 279  H4(M)=HX(J,M)
      GO TO 300
 280  H5(M)=HX(J,M)
      GO TO 300
 284  H9(M)=HX(J,M)
 300  CONTINUE
      READ (5,109) MTIT
      CALL MAPA (7,XX,H2,1,241,WL,WH,VL,VH,10HX DIST(IN),1H ,MTIT,1)
      CALL MAPA (7,XX,H3,1,241,WL,WH,VL,VH,10HX DIST(IN),1H ,MTIT,1)
      CALL MAPA (7,XX,H4,1,241,WL,WH,VL,VH,10HX DIST(IN),1H ,MTIT,1)
      CALL MAPA (7,XX,H5,1,241,WL,WH,VL,VH,10HX DIST(IN),1H ,MTIT,1)
      CALL MAPA (7,XX,H9,1,241,WL,WH,VL,VH,10HX DIST(IN),1H ,MTIT,1)
C
C------PRINT FILM PLOTS
C
      CALL MAPM (6,XX,H2,1,241,WL,WH,VL,VH,XT,YT,MTIT,1)
      CALL MAPM (6,XX,H3,1,241,WL,WH,VL,VH,XT,YT,MTIT,1)
      CALL MAPM (6,XX,H4,1,241,WL,WH,VL,VH,XT,YT,MTIT,1)
      CALL MAPM (6,XX,H5,1,241,WL,WH,VL,VH,XT,YT,MTIT,1)
      CALL MAPM (6,XX,H9,1,241,WL,WH,VL,VH,XT,YT,MTIT,1)
      CALL MAPM (1,XX,H9,1,241,WL,WH,VL,VH,XT,YT,MTIT,1)
      CALL MAPM (2,XX,H2,1,241,WL,WH,VL,VH,XT,YT,MTIT,1)
      CALL MAPM (2,XX,H3,1,241,WL,WH,VL,VH,XT,YT,MTIT,1)
      CALL MAPM (2,XX,H4,1,241,WL,WH,VL,VH,XT,YT,MTIT,1)
      CALL MAPM (2,XX,H5,1,241,WL,WH,VL,VH,XT,YT,MTIT,1)
      CALL MAPM (2,XX,H9,1,241,WL,WH,VL,VH,XT,YT,MTIT,1)
      CALL MAPM (4,XX,H9,1,241,WL,WH,VL,VH,XT,YT,MTIT,1)
```

```
C
      N=N+1
      GO TO (350,351,352),N
 350  DO 360 J=1,IDATA
      DO 360 M=1,MA
 360  HX(J,M)=HY(J,M)
      GO TO 267
 351  DO 361 J=1,IDATA
      DO 361 M=1,MA
 361  HX(J,M)=HXY(J,M)
      GO TO 267
 352  CONTINUE
      DO 400 I=1,IDATA
      HY4(I)=HY4(I)+ABS(HY5(I))
 400  CONTINUE
      READ(5,109) MTI2
      CALL MAPA(7,H1,HY4,1,5,WL,WH,VL,VH,5HDEPTH,3HP-P,MTI2,1)
      CALL MAPA(5,H1,HY4,1,5,WL,WH,VL,VH,5HDEPTH,3HP-P,MTI2,1)
      CALL MAPM(5,H1,HY4,1,5,WL,WH,VL,VH,XXT,YTT,MTI2,1)
 450  CONTINUE
      READ (5,109) MTI3
      CALL MAPA (7,W,HY4,1,5,WL,WH,VL,VH,5HWIDTH,3HP-P,MTI3,1)
      CALL MAPA (5,W,HY4,1,5,WL,WH,VL,VH,5HWIDTH,3HP-P,MTI3,1)
      CALL MAPM (5,W,HY4,1,5,WL,WH,VL,VH,XTT,YTT,MTI3,1)
 500  STOP
C
C-----FORMAT STATEMENTS
C
 100  FORMAT (5X,F5.2)
 101  FORMAT (5X,2F5.3, F10.8)
 102  FORMAT (5X,3I5)
 103  FORMAT (5X,2F5.2)
 104  FORMAT (I10)
 109  FORMAT (8A10)
 110  FORMAT (1H1,5X,23HMAX VALUES FOUND FOR HX,F10.4,3X,6HFOR HY,F10.4)
 111  FORMAT (/////,5X,10HDATA ENTRY,2X,I2,2X,2HOF,I5)
 112  FORMAT (/,5X,7HSIGMA =,F5.2,6X,15HX (MIN./MAX.) =,I5,1H/,I5)
 113  FORMAT (/,5X,36HDISTANCE ABOVE THE SURFACE DEFECT IS,2X,F5.3,2X,3H
     1IN.)
 114  FORMAT (/,5X,33HTHE DEFECT DIMENSION, IN UNITS OF,2X,F5.3,2X,3HIN.
     1)
 115  FORMAT (/,42X,F5.2)
 116  FORMAT (30X,11H-----------,7X,11H-----------,3(/,40X,1H*,7X,1H*),2
     1X,F5.2,2(/,40X,1H*,7X,1H*),/,40X,9H---------)
      END
```

Appendix B

Finite element modeling code.

1. Mesh generation

2. Element ordering

3. Vector potential and flux density
   calculation

```
1        PROGRAM MESH(INPUT,OUTPUT,PUNCH,FILMPL,TAPE5=INPUT,TAPE6=OUTPUT,
         1TAPE8=PUNCH)
C
C
C        **********                                              **********
C
C        PROGRAM MESH GENERATES A PLANAR TWO-DIMENSIONAL TRIANGULAR ELEMENT
C        STRUCTURE WITHIN THE SYMMETRICAL BOUNDARY SHAPE SPECIFIED BY EIGHT
C        GIVEN BOUNDARY POINTS.
C
C        IN THE ORDER OF READING, THE FOLLOWING INPUT DATA IS REQUIRED.
C        ....INITNP AND INITEL ARE THE INITIAL NUMBERING VALUES
C             FOR THE NODAL POINTS AND ELEMENTS RESPECTIVELY,
C             USUALLY 1,1.
C        ....NDIVX AND NDIVY ARE THE NUMBER OF ELEMENTAL
C             DIVISIONS ALONG THE X AND Y AXES RESPECTIVELY.
C        ....XCOR AND YCOR ARE THE (X,Y) COORDINATES OF THE
C             EIGHT DEFINING BOUNDARY POINTS FOR THE GIVEN SHAPE.
C        ....XMIN, XMAX, YMIN, YMAX ARE THE MINIMUM AND MAXIMUM
C             VALUES OF X AND Y ASSOCIATED WITH THE GIVEN SHAPE.
C             (XMAX - XMIN) SHOULD BE EQUAL TO (YMAX - YMIN).
C
C        OUTPUT DATA INCLUDES THE TOTAL NUMBER OF NODE POINTS, THE TOTAL
C        NUMBER OF ELEMENTS, A LISTING OF THE (X,Y) COORDINATES FOR EACH
C        NODE POINT AND THE NODE POINTS DEFINING EACH ELEMENT, TOGETHER
C        WITH A PLOT OF THE MESH STRUCTURE.
C
C        **********                                              **********
C
         DIMENSION XCOR(8),YCOR(8),RN(8),XORD(1250),YORD(1250),NP(2360,3)
C
C        READ AND INITIALIZATION OF DATA
C
         READ(5,1) INITNP,INITEL
         WRITE(6,2)
         WRITE(6,1)INITNP,INITEL
C
         READ(5,3)NDIVX,NDIVY
         WRITE(6,4)
         WRITE(6,3)NDIVX,NDIVY
C
         READ(5,5)(XCOR(I),YCOR(I),I=1,8)
         WRITE(6,6)
         WRITE(6,5)(XCOR(I),YCOR(I),I=1,8)
C
         READ(5,7)XMIN,XMAX,YMIN,YMAX
         WRITE(6,8)
         WRITE(6,7) XMIN,XMAX,YMIN,YMAX
C
         NUMNP=(NDIVX+1)*(NDIVY+1)
         NUMEL=2*(NDIVX)*(NDIVY)
         WRITE(6,13)NUMNP,NUMEL
C
C        CALCULATE NODAL POINT COORDINATES
C
         DX=NDIVX
         DX=1./DX
         DY=NDIVY
         DY=1./DY
C
         IEND=NDIVY+1
         JEND=NDIVX+1
         J1=0
```

```
C
            DO 250 I=1,IEND
            R=(I-1)
            RY=R*DY
C
            DO 240 J=1,JEND
            R=(J-1)
            RX=R*DX
            J1=J1+1
            RN(1)=1.0*(1.-RX)*(1.-RY)*(1.-2.*RX-2.*RY)
            RN(2)=4.0*(RX)*(1.-RX)*(1.-RY)
            RN(3)=-1.0*(RX)*(1.-RY)*(1.-2.*RX+2.*RY)
            RN(4)=4.0*(RX)*(RY)*(1.-RY)
            RN(5)=-1.*(RX)*(RY)*(3.-2.*RX-2.*RY)
            RN(6)=4.*(RX)*(1.-RX)*(RY)
            RN(7)=-1.*(1.-RX)*(RY)*(1.+2.*RX-2.*RY)
            RN(8)=4.0*(1.-RX)*(RY)*(1.-RY)
C
            XORD(J1)=0.
            YORD(J1)=0.
C
            DO 230 K=1,8
            XORD(J1)=XORD(J1)+RN(K)*XCCR(K)
            YORD(J1)=YORD(J1)+RN(K)*YCCR(K)
      230 CONTINUE
      240 CONTINUE
      250 CONTINUE
C
C       CALCULATE NP   ARRAY
C
            I2=0
C
            DO 340 I=1,NDIVY
C
            J1=(I-1)*(NDIVX+1)+1
C
            DO 330 J=1,NDIVX
            I2=I2+2
            I1=I2-1
            J2=J1+1
            J4=J1+(NDIVX+1)
            J3=J4+1
C
            D1=(XORD(J3)-XORD(J1))**2+(YORD(J3)-YORD(J1))**2
            D2=(XORD(J4)-XORD(J2))**2+(YORD(J4)-YORD(J2))**2
C
            IF(D1.GT.D2) GO TO 320
C
            NP(I1,1)=J1
            NP(I1,2)=J3
            NP(I1,3)=J4
C
            NP(I2,1)=J1
            NP(I2,2)=J2
            NP(I2,3)=J3
C
            GO TO 329
C
      320 CONTINUE
```

```
C
      NP(I1,1)=J1
      NP(I1,2)=J2
      NP(I1,3)=J4
C
      NP(I2,1)=J2
      NP(I2,2)=J3
      NP(I2,3)=J4
C
  329 CONTINUE
      J1=J2
  330 CONTINUE
  340 CONTINUE
      DO 1001 I=1,NUMEL
      DO 1001 J=1,3
      NP(I,J)=NP(I,J)+INITNP-1
 1001 CONTINUE
C
C     WRITE STATEMENT
C
      WRITE(6,9)
      IFAC=INITNP-1
      DO 420 I=1,NUMNP
      I1=I+IFAC
C
      WRITE(6,10) I1,XORD(I),YORD(I)
      WRITE(8,14) I1,XORD(I),YORD(I)
  420 CONTINUE
C
      WRITE(6,11)
      IFAC=INITEL-1
      DO 440 I=1,NUMEL
      I1=I+IFAC
      WRITE(6,12)I1,(NP(I,J), J=1,3)
      WRITE(8,15)I1,(NP(I,J),J=1,3)
  440 CONTINUE
C
C     PLOT ROUTINE
C
      CALL SET(0.0,1.0,0.0,1.0,XMIN,XMAX,YMIN,YMAX,1)
C
      DO 480 I=1,NUMEL
C
      I1=NP(I,1)
      I2=NP(I,2)
      I3=NP(I,3)
C
      CALL POINT(XORD(I1),YORD(I1))
      CALL VECTOR(XORD(I2),YORD(I2))
      CALL VECTOR(XORD(I3),YORD(I3))
      CALL VECTOR(XORD(I1),YORD(I1))
C
  480 CONTINUE
```

```
C
      CALL  FRAME
      STOP
C
C     FORMAT STATEMENTS
C
    1 FORMAT(2I10)
    2 FORMAT(20H1    INITNP    INITEL)
    3 FORMAT(2I10)
    4 FORMAT(20H0      NDIVX     NCIVY)
    5 FORMAT(2F10.4)
    6 FORMAT(20H0      XCOR      YCOR)
    7 FORMAT(4F10.4)
    8 FORMAT(40H0      XMIN      XMAX      YMIN      YMAX)
    9 FORMAT(30H0       NP     XCRD     YORD)
   10 FORMAT(I10,2F10.4)
   11 FORMAT(40H0      ELEM     NP(1)     NP(2)     NP(3))
   12 FORMAT(4I10)
   13 FORMAT(*    NUMNP=*,I5,*    NUMEL=*,I5)
   14 FORMAT(I10,20X,2F10.4)
   15 FORMAT(I10,10X,3I10)
      END
```

```
C      PROGRAM ELANP LISTS THE ELEMENTS AROUND EACH NODE POINT INSIDE THE
C      GIVEN BOUNDARY SHAPE.
C      INPUT DATA REQUIRED FOR THE PROGRAM INCLUDES.....
C      ....NUMEL,NST,NED ARE THE TOTAL NUMBER OF ELEMENTS
C           GENERATED FOR THE GIVEN SHAPE BY THE MESH PROGRAM,
C           THE NUMBER OF THE FIRST NODE POINT INSIDE THE
C           GIVEN BOUNDARY AND THE NUMBER OF THE LAST NODE
C           POINT INSIDE THE BOUNDARY RESPECTIVELY.
C      ....A TOTAL LISTING OF THE NODE POINTS DEFINING EACH
C           ELEMENT AS GENERATED BY LINES 420 TO 440 OF PROGRAM
C           MESH.
C
C      OUTPUT DATA CONSISTS OF A LISTING OF EACH NODE POINT BETWEEN NST
C      AND NED WITH A COUNT OF THE NUMBER OF ELEMENTS AROUND EACH NODE
C      POINT AND THEIR IDENTIFICATION.
C
C      THOSE NODE POINTS BETWEEN NST AND NED LYING ON THE BOUNDARY ARE
C      IDENTIFIABLE BY A ROW OF ZEROS AFTER THE NODE NUMBER.
C
C      **********                                           **********
C
       DIMENSION NOP(20),NP(2360,3)
     6 FORMAT(I10,10X,3I10)
     8   FORMAT(3I10)
       READ(5,8) NUMEL,NST,NED
       READ(5,6) (N,NP(N,1),NP(N,2),NP(N,3),NN=1,NUMEL)
       M=0
       DO 42 K=NST,NED
       ICONT=0
       DO 82 IQ=1,14
       NOP(IQ)=0
    82 CONTINUE
       KL=NST-2
       KK=K/KL
       K1=KK*KL+1
       K2=KK*KL
       IF(K .EQ. K1) GO TO 43
       IF(K .EQ. K2) GO TO 43
       DO 50 KX=1,2
       GO TO (90,92),KX
    90 MS=K-K1+M+(KK-1)*2*(NST-3)
       ME=MS+3
       GO TO 94
    92 MS=MS+2*(NST-3)
       ME=MS+3
    94 CONTINUE
       DO 44 I=MS,ME
       IF(NP(I,1) .EQ. K) GO TO 78
       IF(NP(I,2) .EQ. K) GO TO 78
       IF(NP(I,3) .EQ. K) GO TO 78
       GO TO 44
    78 ICONT=ICONT+1
       NOP(ICONT)=I
    44 CONTINUE
    50 CONTINUE
       M=M+1
       NSSSS=NST-5
       IF(M .GT. NSSSS) M=0
    43 WRITE(6,80) K,ICONT,(NOP(N),N=1,14)
       WRITE(8,80) K,ICONT,(NOP(N),N=1,14)
    42 CONTINUE
    80 FORMAT(16I5)
       STOP
```

```
      PROGRAM POTEN(INPUT,OUTPUT,FILMPL,TAPE5=INPUT,TAPE6=CUTPUT)
C
C     **********                                              **********
C
C     PROGRAM POTEN IS A FINITE ELEMENT ALGORITHM WHICH CALCULATES THE
C     VECTOR POTENTIAL AT EVERY NODE OF THE REGION DISCRETIZED INTO
C     TRIANGULAR ELEMENTS BY PROGRAM MESH.
C     POTEN IS BASED ON ANDERSONS EQUATIONS (REF.32) AND REQUIRES INPUT
C     DATA FROM BOTH THE MESH AND ELANP PROGRAMS AS WELL AS A MODEL OF
C     THE B/H CHARACTERISTIC CF THE FERROMAGNETIC MATERIAL AND THE
C     BARS CURRENT DENSITY.
C
C     IN GENERAL THE PROGRAM HAS TO BE WRITTEN FCR THE PARTICULAR
C     GEOMETRY UNDER CONSIDERATION AND THE REQUIRED OUTPUT.
C
C     INPUT DATA REQUIRED INCLUDES --
C     .....NUMBGN,NUMDIV DEFINE THE SCANNING PATH FOR THE FLUX DENSITY
C          PLOTS
C     .....NUMNP,NUMEL ARE THE TOTAL NUMBER OF NODE POINTS AND ELEMENTS
C          RESPECTIVELY
C     .....NAROS AND NAROE CORRESPOND TO NST AND NED IN THE ELANP
C          PROGRAM
C     .....THE LAST THREE READ STATEMENTS REFER TO THE DATA GENERATED
C          BY MESH AND ELANP PROGRAMS
C     .....RVPER IS THE INVERSE OF THE PERMEABILITY CF FREE SPACE
C     .....CURR IS THE BAR CURRENT DENSITY
C
C     **********                                              **********
C
      DIMENSION NP(1160,3),CJ(1160),RMU(1160),SL(1160,6),MAT(1160)
     1          ,A(630),XORD(630),YORC(630),AREA(1160),BX(1160),BY(1160)
     2          ,B(1160),IEDG(630),IETG(630,8),BXC(50),BYC(50),BC(50)
     3          ,XX(50)
C
C     INPUT DATA
C
      READ (5,1) NUMBGN,NUMDIV
      READ(5,2) NUMNP,NUMEL,NAROS,NAROE
      READ(5,4) (N, A(N),XORD(N),YORC(N),NN=1,NUMNP)
      READ(5,6) (N,NP(N,1),NP(N,2),NP(N,3),NN=1,NUMEL)
      READ(5,8)(N,IEDG(N),(IETG(N,I),I=1,8),NN=NAROS,NAROE)
C
      RVPER=795774.7155
      CURR=2.6016E+05
C
C     SCALING AND ELEMENT CALCULATIONS
C
      DO 20 I=1,NUMNP
      XORD(I)=XORD(I)*.0254
      YORD(I)=YORD(I)*.0254
   20 CONTINUE
```

```
C
      DO 38 I=1,NUMEL
      IP=NP(I,1)
      JP=NP(I,2)
      KP=NP(I,3)
      XJ=XORD(JP)-XORD(IP)
      YJ=YORD(JP)-YORD(IP)
      XK=XORD(KP)-XORD(IP)
      YK=YORD(KP)-YORD(IP)
      AREA(I)=(XJ*YK-XK*YJ)/2.0
      A1=-(YK-YJ)/2.0
      B1=YK/2.0
      C1=-YJ/2.0
      D1=(XK-XJ)/2.0
      E1=-XK/2.0
      F1=XJ/2.0
      SL(I,1)=(A1*A1+D1*D1)/AREA(I)
      SL(I,2)=(B1*B1+E1*E1)/AREA(I)
      SL(I,3)=(C1*C1+F1*F1)/AREA(I)
      SL(I,4)=(A1*B1+D1*E1)/AREA(I)
      SL(I,5)=(A1*C1+D1*F1)/AREA(I)
      SL(I,6)=(B1*C1+E1*F1)/AREA(I)
   38 CONTINUE
C
C
C        INITIALIZATION OF AIR AND IRON REGICNS
C                -- CALCULATION OF BAR CURRENT
C
      DO 60 I=1,NUMEL
      RMU(I)=RVPER
      CJ(I)=0.0
      MAT(I)=0
   60 CONTINUE
C
      IEBL=301
   66 CONTINUE
      IEBR=IEBL+23
      DO 67 I=IEBL,IEBR
  661 CJ(I)=AREA(I)*CURR
  662 B(I)=1.65
  663 RMU(I)=2019.66
  664 MAT(I)=I
   67 CONTINUE
      IEBL=IEBL+48
      IF (IEBL.LE.852)  GO TO 66
C
C-----CRACK PORTION
C
      DO 68 I=791,794
      RMU(I)=RVPER
      CJ(I)=0.0
      MAT(I)=0
   68 CONTINUE
      DO 69 I=839,842
      RMU(I)=RVPER
      CJ(I)=0.0
      MAT(I)=0
   69 CONTINUE
```

```
C
C          SELECTION OF ACCELERATION FACTOR
C
          ITER=0
          FAC=2.1
          RFAR=0.07
   70     CONTINUE
          IFLAG=0
          ACK=0.0
          ITER=ITER+1
          IF (ITER.EQ.6) GO TO 71
          FAC=FAC-0.2
          GO TO 72
   71     FAC=1.0
   72     CONTINUE
C
C          BEGINING OF ITERATION
C
          DO 326 KOA=1,40
          DO 42 K=NAROS,NAROE
          IF(IEDG(K))201,42,201
  201     T1=T2=T3=0.0
          ME=IEDG(K)
          DO 44 JJ=1,ME
          I=IETG(K,JJ)
          IF(NP(I,1)-K) 77,78,77
   77     IF(NP(I,2)-K) 79,80,79
   79     IF(NP(I,3)-K) 44,82,44
   78     IP=1
          JP=4
          KP=5
          I1=NP(I,2)
          I2=NP(I,3)
          GO TO 84
   80     IP=2
          JP=6
          KP=4
          I1=NP(I,3)
          I2=NP(I,1)
          GO TO 84
   82     IP=3
          JP=5
          KP=6
          I1=NP(I,1)
          I2=NP(I,2)
   84     T1=T1+CJ(I)
          T2=T2+RMU(I)*SL(I,IP)
          T3=T3+RMU(I)*(A(I1)*SL(I,JP)+A(I2)*SL(I,KP))
   44     CONTINUE
          T1=T1/3.0
          AZ=(T1-T3)/T2
          ANEW=A(K)+FAC*(AZ-A(K))
          IF (ABS(A(K)-ANEW).LE.0.0001) GO TO 41
          IFLAG=1
          ACK=ABS(A(K)-ANEW)
   41     CONTINUE
          A(K)=ANEW
   42     CONTINUE
          KMA=(KOA/2)*2
          IF(KMA .NE. KOA) GO TO 326
```

```
C
C         CALCULATION OF NEW FLUX DENSITY IN THE MATERIAL
C
          DO 52 I=1,NUMEL
          IF(MAT(I)-0) 203,52,203
      203 IP=NP(I,1)
          JP=NP(I,2)
          KP=NP(I,3)
          BX(I)=(A(IP)*(XORD(KP)-XORD(JP))+A(JP)*(XORD(IF)-XCRC(KP))+A(KP)*(
         1XORD(JP)-XORD(IP)))/(2.*AREA(I))
          BY(I)=(A(IP)*(YORD(KP)-YORC(JP))+A(JP)*(YORC(IP)-YCRC(KP))+A(KP)*(
         2YORD(JP)-YORD(IP)))/(2.*AREA(I))
          B(I)=SQRT(BX(I)*BX(I)+BY(I)*BY(I))
C
C         CALCULATION OF NEW PERMEABILITY USING MCDELEC B/H CURVE
C
          IF(B(I)-1.3) 91,91,204
      204 IF(B(I)-1.9) 93,93,205
      205 IF(B(I)-2.2) 95,95,206
      206 IF(B(I)-2.5) 97,97,207
      207 RR1=RVPER
          GO TO 99
       91 RR1=95.0+240.5576923*B(I)
          GO TO 99
       93 RR1=B(I)*(89623.82-B(I)*(74098.4562-20369.373*B(I)))-35628.365
          GO TO 99
       95 RR1=6875.0+61628.78767*(B(I)-1.9)
          GO TO 99
       97 RR1=25363.6363+179454.5457*(B(I)-2.2)
       99 RMU(I)=RMU(I)+RFAR*(RR1-RMU(I))
       52 CONTINUE
      326 CONTINUE
C
          IF (ITER.EQ.6) GO TO 350
          IF (IFLAG.EQ.1) GO TO 70
      350 CONTINUE
          WRITE (6,101) ITER,ACK
C
C
C         CALCULATION OF NEW FLUX DENSITY IN AIR PORTION
C
          DO 3500 I=1,NUMEL
          IF (MAT(I)-0) 3500,400,3500
      400 IP=NP(I,1)
          JP=NP(I,2)
          KP=NP(I,3)
          BX(I)=(A(IP)*(XORD(KP)-XORC(JP))+A(JP)*(XORD(IP)-XCRC(KP))+A(KP)*(
         1XORD(JP)-XORD(IP)))/(2.*AREA(I))
          BY(I)=(A(IP)*(YORD(KP)-YORD(JP))+A(JP)*(YORC(IF)-YORC(KP))+A(KP)*(
         2YORD(JP)-YORD(IP)))/(2.*AREA(I))
     3500 CONTINUE
```

```
C
C         CALCULATION OF MAGNETIC FIELD ABOVE BAR
C
          ICONT=0
          NUMEND=NUMBGN+NUMDIV*2-1
          DO 510 I=NUMBGN,NUMEND,2
  410     ICONT=ICCNT+1
          BXC(ICONT)=(BX(I)+BX(I+1))/2.
          BYC(ICONT)=(BY(I)+BY(I+1))/2.
          BC(ICONT)=SQRT(BXC(ICONT)*BXC(ICONT)+BYC(ICCNT)*BYC(ICCNT))
           XX(ICONT)=XORD(ICONT)
  510     CONTINUE
C
C         OUTPUT DATA AND PLOTS
C
          CALL MAPA (7,XX,BXC,1,24,WL,WH,VL,VH,1H ,1H ,1H ,1)
          CALL MAPA (5,XX,BXC,1,24,WL,WH,VL,VH,1H ,1H ,1H ,1)
          CALL MAPM (5,XX,BXC,1,24,WL,WH,VL,VH,1H ,1H ,1H ,1)
          CALL MAPA (7,XX,BYC,1,24,WL,WH,VL,VH,1H ,1H ,1H ,1)
          CALL MAPA (5,XX,BYC,1,24,WL,WH,VL,VH,1H ,1H ,1H ,1)
          CALL MAPM (5,XX,BYC,1,24,WL,WH,VL,VH,1H ,1H ,1H ,1)
          CALL MAPA (7,XX,BC ,1,24,WL,WH,VL,VH,1H ,1H ,1H ,1)
          CALL MAPA (5,XX,BC ,1,24,WL,WH,VL,VH,1H ,1H ,1H ,1)
          CALL MAPM (5,XX,BC ,1,24,WL,WH,VL,VH,1H ,1H ,1H ,1)
C
C         WRITE STATEMENT
C
          WRITE (6,10)
          WRITE (6,12) (MAT(I),I=1,NUMEL,2)
          WRITE (6,10)
          NUMB=1
          DO 550 J=1,25
          NUME=NUMB+12
          WRITE (6,11) (A(I),I=NUMB,NUME)
          NUMB=NUMB+25
  550     CONTINUE
          NUMB=14
          DO 560 J=1,25
          NUME=NUMB+11
          WRITE (6,14) (A(I),I=NUMB,NUME)
          NUMB=NUMB+25
  560     CONTINUE
          STOP
C
C         FORMAT STATEMENT
C
    1     FORMAT (2I10)
    2     FORMAT(4I10)
    4     FORMAT(I10,10X,3F10.4)
    6     FORMAT(I10,10X,3I10)
    8     FORMAT(10I5)
   10     FORMAT (1H1)
   11     FORMAT  (1X,13E10.3)
   12     FORMAT (24I4)
   14     FORMAT (3X,12(1E11.4))
   16     FORMAT (1X,I10,10X,3E16.6)
  101     FORMAT (1X,I10,E15.6)
  102     FORMAT(5X,6(1X,F8.5))
  106     FORMAT(///)
          END
```